Single-cell transcriptome reveals the heterogeneity of malignant ductal cells and the prognostic value of REG4 and SPINK1 in primary pancreatic ductal adenocarcinoma

Yutian Ji[1,2,3], Qianhui Xu[4] and Weilin Wang[1,2,3]

[1] Department of Hepatobiliary and Pancreatic Surgery, The Second Affiliated Hospital, Zhejiang University School of Medicine, Hangzhou, Zhejiang, China
[2] Zhejiang University School of Medicine, Hangzhou, Zhejiang, China
[3] Key Laboratory of Precision Diagnosis and Treatment for Hepatobiliary and Pancreatic Tumor of Zhejiang Province, Hangzhou, China
[4] Fudan University, Shanghai, China

ABSTRACT

Background. Pancreatic ductal adenocarcinoma (PDAC) is one of the leading causes of cancer-related deaths, with very limited therapeutic options available. This study aims to comprehensively depict the heterogeneity and identify prognostic targets for PDAC with single-cell RNA sequencing (scRNA-seq) analysis.

Methods. ScRNA-seq analysis was performed on 16 primary PDAC and three adjacent lesions. A series of analytical methods were applied for analysis in cell clustering, gene profiling, lineage trajectory analysis and cell-to-cell interactions. *In vitro* experiments including colony formation, wound healing and sphere formation assay were performed to assess the role of makers.

Results. A total of 32,480 cells were clustered into six major populations, among which the ductal cell cluster expressing high copy number variants (CNVs) was defined as malignant cells. Malignant cells were further subtyped into five subgroups which exhibited specific features in immunologic and metabolic activities. Pseudotime trajectory analysis indicated that components of various oncogenic pathways were differentially expressed along tumor progression. Furthermore, intensive substantial crosstalk between ductal cells and stromal cells was identified. Finally, genes (REG4 and SPINK1) screened out of differentially expressed genes (DEGs) were upregulated in PDAC cell lines. Silencing either of them significantly impaired proliferation, invasion, migration and stemness of PDAC cells.

Conclusions. Our findings offer a valuable resource for deciphering the heterogeneity of malignant ductal cells in PDAC. REG4 and SPINK1 are expected to be promising targets for PDAC therapy.

Subjects Bioinformatics, Cell Biology, Genetics, Molecular Biology, Oncology

Keywords Single-cell transcriptome, Pancreatic ductal adenocarcinoma, Ductal cell, Immune microenvironment, Metabolic reprogramming, Prognostic biomarker

Submitted 12 December 2023
Accepted 17 April 2024
Published 28 May 2024

Corresponding author
Weilin Wang, wam@zju.edu.cn

Academic editor
Joseph Gillespie

Additional Information and Declarations can be found on page 21

DOI **10.7717/peerj.17350**

How to cite this article Ji Y, Xu Q, Wang W. 2024. Single-cell transcriptome reveals the heterogeneity of malignant ductal cells and the prognostic value of REG4 and SPINK1 in primary pancreatic ductal adenocarcinoma. *PeerJ* **12**:e17350 http://doi.org/10.7717/peerj.17350

INTRODUCTION

Pancreatic ductal adenocarcinoma (PDAC), one of the most aggressive and fatal diseases with a current 5-year survival rate less than 10%, accounts for approximately 90% of malignant pancreatic diseases (*Siegel et al., 2022*). Surgical resection remains the main choice for PDAC patients. However, most of them are diagnosed at advanced stage, losing the opportunity to receive a surgery (*Winter et al., 2012*; *Gobbi et al., 2013*; *Ryan, Hong & Bardeesy, 2014*). Although multiple novel therapies have been beneficial with different types of solid tumors, very few treatment modalities have shown promising efficacy in PDAC (*Tempero et al., 2019*; *Sohal et al., 2021*; *Hosein et al., 2022*). A primary reason for the observed treatment recalcitrance and high mortality rate is owing to its complicated intratumoral heterogeneity and intensive cellular crosstalk (*Moffitt et al., 2015*; *Ho, Jaffee & Zheng, 2020*).

Previous genomic and transcriptomic studies have revealed that critical gene mutations or aberrant signaling pathways driving the pathogenesis of PDAC, such as KRAS (over 90%), TP53, SMAD4 and CDKN2A (over 50%) (*Australian Pancreatic Cancer Genome Initiative et al., 2012*; *Witkiewicz et al., 2015*). Other novel recurrent mutations (<10%) have also been identified from unbiased analyses of PDAC. These diverse mutations converge on specific pathways and processes, including KRAS, TGF-β, WNT, Notch signaling, chromatin remodeling and DNA repair pathways (*Australian Pancreatic Cancer Genome Initiative et al., 2015*; *Raphael et al., 2017*). Also, deep insights have been gained regarding the immunologic and metabolic reprogramming in PDAC progression (*Yao, Maitra & Ying, 2020*). The diversity of stromal and immune cell types comprises a quite complicated tumor microenvironment (TME) in PDAC (*Teng et al., 2015*; *Ligorio et al., 2019*; *Ho, Jaffee & Zheng, 2020*; *Steele et al., 2020*). Meanwhile, prominent metabolic adaptions, usually reflected as the 'Warburg effect', are one of the hallmarks of pancreatic cancer cells (*Warburg, Wind & Negelein, 1927*). Except for the enhanced glycolysis, multiple other metabolic activities, like fatty acid metabolism, steroid biosynthesis and glutamine synthesis, are largely altered in PDAC as well (*Daemen et al., 2015*; *Karasinska et al., 2020*).

In the past decades, some major breakthroughs in PDAC treatment have been made for a small fraction of patients based on bulk mRNA sequencing (*Oettle et al., 2013*; *Heining et al., 2018*; *Katz et al., 2021*). Unfortunately, most PDAC patients have not benefited from our current knowledge of the genetics and biology on PDAC yet, due to the limited picture of cellular complexity provided by bulk profiling technologies (*Yao, Maitra & Ying, 2020*). Recent advances in single-cell genomics have enabled us to conduct in-depth analyses of tumoral heterogeneity at unprecedented molecular resolutions (*Tanay & Regev, 2017*). It has effectively recognized multiple evolutionary lineages and cellular subpopulations, as well as their relative crosstalk within the TME. To date, a series of novel molecular subtype classifications has been developed for PDAC based on scRNA-seq (*Ligorio et al., 2019*; *Elyada et al., 2019*; *Hosein et al., 2019*; *Peng et al., 2019*; *Lin et al., 2020*; *Lee et al., 2021*), which has complemented the original binary classification including classical and basal-like subtypes (*Collisson et al., 2019*). In addition to tumor cells, other stromal cells

shaping the TME complexity were also classified into different components with specific gene expression patterns.

Here, we applied scRNA-seq analysis to dissect the intratumoral heterogeneity during PDAC progression. The transcriptome profile of a total of 32,480 cells from 16 primary PDAC tumors and three adjacent tissues was acquired. We found that PDAC tumor mass was highly heterogeneous and composed of diverse malignant and stromal cell types. Further, malignant ductal cells were distinguished into five subgroups by featured gene expression and biological profiles. Significant gene expression alterations which related to known tumor-related signaling pathways were identified as well. In addition, we also described intricate multicellular crosstalk in the TME. Therefore, our study delineates a comprehensive understanding of the single-cell transcriptome landscape in human primary PDAC and may hopefully provide a resource for further investigations aimed at characterizing and targeting specific populations in PDAC.

MATERIALS & METHODS

Information of single-cell datasets

The sequencing information of 32,480 single cells from 16 treatment-naive primary PDAC tumors and three adjacent tissues (detailed in Tables S1, S2) was acquired from the Gene Expression Omnibus (GEO) database (GSE155698) (*Steele et al., 2020*). Detailed parameters of gene-barcode matrices, feature data, as well as unique molecular identifier (UMI) count tables were illustrated in published works (*Li et al., 2017*). All information applied in our study is publicly available and open access.

ScRNA sequencing data processing

Data processing of scRNA sequencing in our study was performed as described previously (*Xu et al., 2021a*). Briefly, Seurat (v2.3.0) R toolkit with the Read 10× () function was applied to import the Seurat object containing gene expression data (*Satija et al., 2015*). Quality control was conducted before the subsequent analysis of scRNA-seq data. All functions were run with default parameters, unless specified otherwise. Gene-cell matrices were filtered to exclude unqualified cells (<500 transcripts/cell, >30% mitochondrial genes) and genes (<300 cells/gene and >25,000 cells/gene). Each sample was represented as a fraction of the gene multiplied by 10,000, then transformed into a natural logarithm and normalized after adding one to avoid taking the logarithm of zero.

Cell clustering and annotation

The Seurat package implemented in R was applied to identify major cell types. Principal component analysis (PCA) was conducted using the top 2,000 highly variable genes (HVGs) derived from the normalized expression matrix (Fig. S3A). Principal components (PCs) whose estimated *P* value less than 0.05 were selected and the optimal resolution was determined by the cluster tree algorithm (Fig. S3B). Additional screening methods (DoubletFinder and CellCycleScoring) were performed to exclude unqualified cells for subsequent analysis (Figs. S4A, S4B). t-distributed Stochastic Neighbor Embedding (t-SNE) analysis was performed to visualize the clustering of single cells. The cluster distribution

of single cells from each sample was presented (Fig. S4D). Genes specific for each cluster were determined with FindAllMarkers based on the normalized gene expression data. 'Find.markers' was conducted in identifying the DEGs in different clusters. DEGs and literature-known markers were used to define the cell groups (Table S3).

CNV assessment in single cells

InferCNV R package (version 1.4.0) was applied to estimate CNV of single cells (*Patel et al., 2014*). Various parameters were used to evaluate the inferCNV analysis, including "denoise", default hidden Markov models (HMMs), and a value of 0.1 for "cutoff". The default Bayesian latent mixture model with a threshold of 0.0005 was performed to assess the posterior probabilities of CNV alterations to minimize false-positive CNV calls.

Identification of DEGs and pathways

Wilcoxon Rank-Sum Test with FindMarkers function (adjusted P-value <0.05, only.pos = TRUE and logFC.threshold = 0.25) was used to determine the DEGs within each cluster. Analysis for alterations in hallmark oncogenic and metabolic pathways was predominantly conducted with MSigDB databases (https://www.gsea-msigdb.org/gsea/msigdb) (*Liberzon et al., 2011*). Then, the gene set variation analysis (GSVA) package (version 1.36.3) (*Hänzelmann, Castelo & Guinney, 2013*) was used to estimate relative pathway activities in different ductal cell clusters.

Pseudotime trajectory analysis for single cells

Using Monocle2 (v2.16.0) (*Trapnell et al., 2014*), single-cell pseudotime trajectory analysis was performed to investigate cell state transitions under the assumption that one-dimensional 'time' could delineate the high-dimensional expression values. The previously identified malignant cell cluster was loaded into R environment. The newCellDataSet function was conducted to create an object with the parameter expressionFamily = negbinomial.size. Genes qualifying for our standards (mean_expression $\geq$ 0.1 and dispersion_empirical $\geq$ 1 * dispersion_fit identified) were filtered for the trajectory analysis. Dimension reduction was achieved using reduceDimension() with parameters reduction_method = "DDRTree" and max_components = 2. Meanwhile, minimum spanning trees were plotted using visualization function "plot_cell_trajectory". "DifferentialGeneTest" and "plot_pseudotime_heatmap" were applied respectively to estimate and visualize gene expression changes following the pseudotime trajectory, and then genes were grouped into subclusters based on their expression profiles. Gene expression patterns (detailed in Table S4) were utilized to group genes into subgroups. Genes derived from Branch Expression Analysis Modeling (BEAM) analysis (with a q-value <0.05) were grouped and plotted with "plot_genes_branched_heatmap()" function (detailed in Table S5).

Cell-to-cell interaction analysis

Cells defined as malignant ductal cells, macrophages, T cells, B cells, dendritic cells, monocytes, NK cells and cancer-associated fibroblasts (CAFs) in our analysis were input to CellPhoneDB (version 2.1.7) for exploring potential cell-to-cell interactions among

them (*Efremova et al., 2020*). Then, receptors and ligands respectively expressed in more than 10% of cells in the corresponding subclusters were identified as the most relevant cell type-specific interactions.

As for pairwise comparisons, cluster labels of all cells were firstly permuted randomly for 1,000 times to obtain the average expression levels of the receptors and ligands among interacting clusters, after which a null distribution was generated for each receptor–ligand pair. Then, ultimate results for cell-to-cell interactions were determined by measuring *P* values, which were obtained by comparing the proportion of the means that were higher than the actual mean, for the probability of the cell-type specificity of the corresponding receptor and ligand.

Validation of gene expression

Three primary human pancreatic cancer cell lines (BXPC-3, CAPAN-2 and Mia-PACA2) and the normal pancreatic ductal cell line (HPNE) were purchased from the Cell Bank of the Type Culture Collection of the Chinese Academy of Sciences, Shanghai Institute of Biochemistry and Cell Biology. The purity of cells used in our experiment was verified by short-tandem repeat (STR) polymorphism analysis and mycoplasma was regularly tested to avoid mycoplasma contamination. BXPC-3 and CAPAN-2 were cultured in RPMI 1640 (Cat. No. 11875093; Gibco, Waltham, MA, USA), while MIA-PACA2 and HPNE were cultured in DMEM (Cat. No. 11965092; Gibco, Waltham, MA, USA), both with 10% fetal bovine serum (FBS; Cat. No. 16000-044; Gibco, Waltham, MA, USA). Cells were cultured in a humidified atmosphere of 5% CO2 and 95% relative humidity at 37 °C.

Quantitative real-time PCR (qRT-PCR) was performed for mRNA quantification. qRT-PCR results in triplicates were analyzed as described previously (*Xu et al., 2021b*). The relative expression of potential prognostic genes was measured with the $2^{-\Delta\Delta Ct}$ method, with 18S levels as an endogenous control. Primer sequences of above genes were listed: REG4, 5′-TGAGGAACTGGTCTGATGCCGA-3′ and 5′-TCCATATCGGCTGGCTTCTCTG-3′; SPINK1, 5′-ATGACCCTGTCTGTGGGACTGA-3′ and 5′-GCGGTGACCTGATGGGATTTCA-3′; and 18S, 5′-ACCCGTTGAACCCCATTCGTGA-3′ and 5′-GCCTCACTAAACCATCCAATCGG-3′.

As for protein levels, cells were lysed in lysis buffer (Cat. No. G2002; Servicebio, Beijing, China) in the presence of protease inhibitor cocktail (Cat. No. P2714; Sigma, Burlington, MA, USA). Cell lysates were then subjected to western blotting as previously described (*Cui et al., 2020*). Primary antibodies were used as follows: REG4 (Cat. No. ab255820; Abcam, Cambridge, UK), SPINK1 (Cat. No. ab183034; Abcam, Cambridge, UK), and GAPDH (Cat. No. 10494-1-AP; Proteintech, Chicago, IL, USA). SuperSignal West Pico PLUS Chemiluminescent Substrate (Thermo Fisher, Waltham, MA, USA, Cat. No. 34577) was used for chemiluminescence staining. Bio-Rad ChemiDoc Imaging System was utilized for chemiluminescence detection.

In addition, Kaplan–Meier survival analysis was detected with Gene Expression Profiling Interactive Analysis (GEPIA, http://gepia.cancer-pku.cn) (*Tang et al., 2017*). Immunohistochemistry (IHC) images were obtained from Human Protein Atlas (HPA, https://www.proteinatlas.org/) (*Uhlén et al., 2015*).

Analysis for immune infiltration

Tumor Immunity Estimation Resource (TIMER, https://cistrome.shinyapps.io/timer) (*Li et al., 2016*) was used to analyze the correlation between gene expression and immune infiltrating cell types. The purity-corrected partial Spearman's correlation coefficient was used to evaluate the relationship between gene expression and immune infiltration.

Cell transfection

pGMLV-REG4-shRNA-puro and pGMLV-SPINK1-shRNA-puro plasmids were purchased from Genomeditech (Shanghai, China). HEK-293T cells were transfected with psPAX2, pVSVG and lentiviral plasmids to produce lentiviruses. Virus particles were collected from supernatants and filtered through a 0.45 μm filter. MIA-PACA2 cells were infected by indicated viruses, followed by puromycin selection for 3 weeks, to construct stable cell lines.

Cell proliferation assay

Cell Counting Kit-8 (CCK-8, MCE, Cat. No. HY-K0301) was used to detect cell proliferation. Cells after transfection were seeded in 96-well plates at a density of 4000 cells/well, and incubated overnight for adherence. Cells were cultured in the presence/absence of 50 nM gemcitabine hydrochloride (MCE, Cat. No. HY-B0003). CCK-8 reagent was added into wells after 0, 24, 48, 72 h, following incubation for 2 h at 37 °C, as recommended by instructions. Cell absorbance was detected with a microplate reader at 450 nm.

Colony formation assay

Cells were seeded in 6-well plates at a density of 1,000 cells/well. Then they were cultured for 10 days in the incubator, with culture medium replacement every 3 days. At day 10, cell colonies were fixed with 4% paraformaldehyde for 10 min and stained with 0.1% crystal violet for 15 min. The number of colonies (>50 cells per colony) was counted under microscopy.

Wound healing assay

To examine cell migration, cells were seeded in 6-well plates at a density of 6×10^5 cells/well. Then they were cultured in the incubator until cells were covered almost confluent. The surface of cells was scratched by the tip of a 200 μL pipette and washed twice with PBS. Cell images were captured with microscopy immediately and 20 h later.

Sphere formation assay

Tumor spheroids were created with a hanging drop method (*Honeder et al., 2021*). Cells after transfection were suspended at a concentration of 5×10^4 cells/mL in culture medium containing 3 μg/mg type I collagen (Cat. No. 354236; Corning, Corning, NY, USA). 20 μL droplets were transferred to the lid of 100 mm dishes and were inverted over dishes containing 5 mL phosphate buffer solution (PBS) to avoid drying. About 8 days later, spheroids were observed under microscopy and their diameters were measured.

Data analysis

All statistical analyses for scRNA-seq data were carried out with R (http://www.r-project.org). Not each of the data points was presented in all box and violin plots due to the fact that extensive data points would obscure overall distribution. A two sided paired or unpaired Student's *t*-test and unpaired Wilcoxon rank-sum test were performed in the cases indicated. For *in vitro* experiments, data from three independent experiments were expressed as the mean ± SEM and analyzed using GraphPad Prism 7. The relative protein levels were measured with Fiji Is Just Image J (FIJI, win32). Statistical significance was defined as a P value <0.05.

RESULTS

Single-cell atlas in primary PDAC

To understand the diversity in the TME of PDAC, 16 samples diagnosed with primary PDAC and three adjacent pancreatic tissues were included for scRNA-seq analysis. For unbiased clustering, 26 main cell clusters were identified at first (Table S3). The cluster distribution of single cells from each patient was presented (Figs. S3C, S3D). According to cell expression patterns and known markers, cells were further optimized to six clusters with differential gene expression profiles, including ductal cells, myeloid cells, T cells, B cells, NK cells and CAFs (Fig. 1A). In most cases, multiple well-known markers were used to identify cell clusters, such as KRT19 and TSPAN8 for ductal cells, AIF1 and FPR1 for myeloid cells, CD2 and CD3 for T cells, CD79 for B cells, NKG7, GNLY, KLRD1 for NK cells, and COL1A1 and COL1A2 for CAFs (Fig. 1B). In general, we observed a distinct increase in the proportion of ductal and B cell clusters in PDAC samples compared to adjacent tissues, while a decrease in the proportion of NK cells (Fig. 1C). Meanwhile, 16 PDAC samples shared similarities in cell type composition, while the relative proportion of each cell cluster exhibited a big discrepancy (Fig. 1D), which reflects both the tumoral heterogeneity and similarity across PDAC patients.

CNV landscape distinguishing malignant ductal cells in PDACs

To investigate malignant status of cells, large-scale chromosomal CNVs were defined in single cells by inferCNV. A clustered heatmap was generated across samples (Fig. 2A). Ductal cells exhibited remarkably higher CNV levels than other cell types. CAFs presented moderate CNV levels. CNVs in ductal cells and CAFs were both significantly higher in PDAC than those in adjacent tissues (Figs. 2B, 2C). These results demonstrated that ductal cells were the most predominantly malignant cells in PDAC, which were also supported by the specific expression of poor prognosis markers KRT19 and TSPAN8 mentioned above. Ductal cells in PDAC samples expressing relatively high CNVs, with immune cells as references, were screened out and defined as 'malignant cells' for subsequent analysis.

Distinct subgroups in malignant cells

Malignant cells identified above were further analyzed and clustered into five subtypes according to t-SNE analysis (Fig. 3A, Fig. S5A). By comparing gene expression levels, we found that each subgroup expressed its specific gene set which could be distinguished from

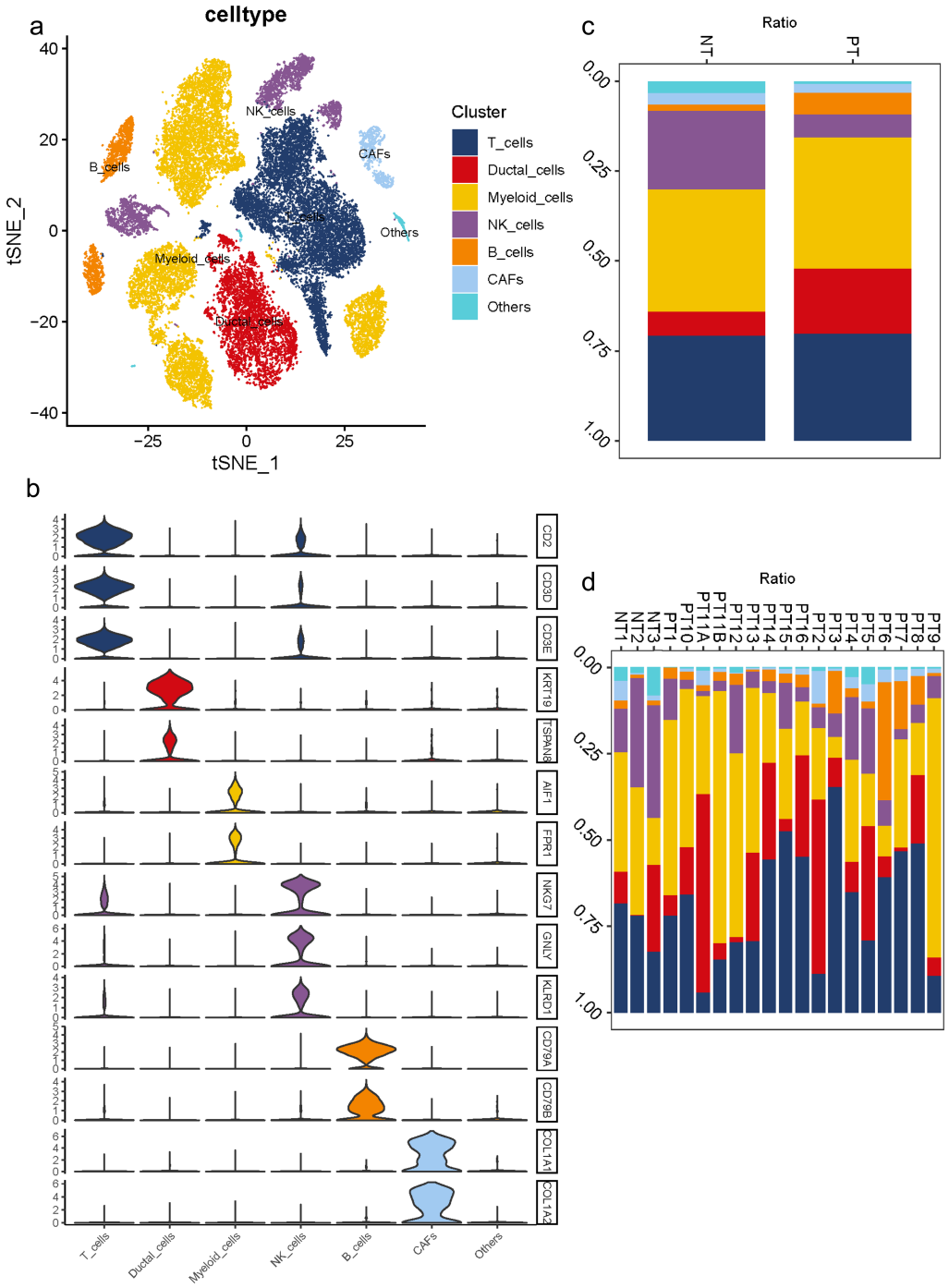

Figure 1 **Diverse cellular subclusters in primary PDAC analyzed by single-cell transcriptomics.** (A) Six main cell types identified in primary PDAC lesions. (B) Signature genes across six subtypes presented on violin plots. (C) Cell cluster proportions between adjacent normal tissues and primary PDAC lesions. (D) Cell cluster proportions across 19 samples.

Full-size DOI: 10.7717/peerj.17350/fig-1

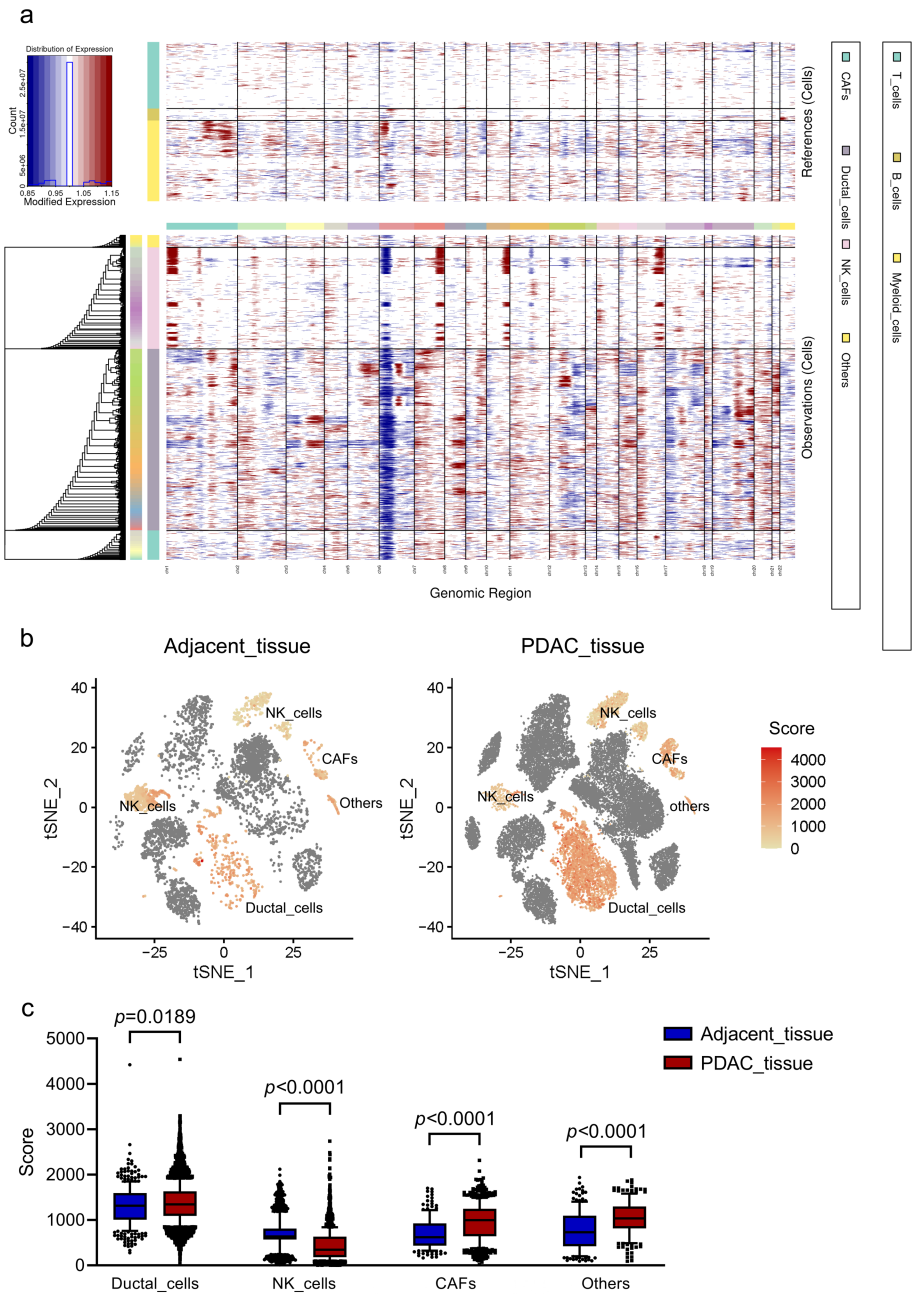

Figure 2 **CNV analysis in different cell clusters in primary PDAC.** (A) A hierarchical heatmap of large-scale CNVs of 16 PDAC samples and 3 adjacent normal tissues. (B) Specific distributions of CNV scores in different cell clusters. (C) CNV scores in cell clusters depicted by box plots.

Full-size DOI: 10.7717/peerj.17350/fig-2

each other. Notably, subgroup 1 was the major population presented in malignant cells with high levels of MMP7 and DEFB1; subgroup 2 exhibited high levels in CEACAM5 and CLDN18; subgroup 3 were mainly characterized by CA2 and GPX2; subgroup 4 specifically expressed FXYD2 and AMBP; and RGS13 and AZGP1 were uniquely expressed

in subgroup 5 (Fig. 3B). The specific distribution of each cell marker expression in single cells was presented (Fig. 3C).

To further describe the biological functions of malignant subgroups, GSVA was conducted in the following analysis (Fig. 3D, Fig. S5B). Generally, genes from multiple classical oncogenic pathways were enriched in almost each subgroup (*Hezel et al., 2006*), further confirming their malignancy. In particular, subgroup 1 was enriched for genes from ERBB signaling pathway. Genes from MYC, WNT/β-catenin and PI3K/AKT/MTOR pathways were enriched in subgroup 2. Subgroup 3 was enriched for MAPK and Notch pathways. Subgroup 5 was enriched for genes from P53 signaling pathway. In addition, gene expression patterns in subgroup 2, 3 and 4 were also related to KRAS pathway, which is the most frequently mutated pathway in PDAC. Also, commonly reported cellular biological and metabolic activity alterations were also detected in each subgroup specifically (*Yao, Maitra & Ying, 2020*). For instance, subgroup 1 showed heightened activities of unfolded protein response (UPR) and reactive oxygen species (ROS) pathway. Genes for subgroup 2 exhibited high enrichment involved in glycose and lipid metabolism, such as glycolysis and adipogenesis, which suggested the elevated energy requirements during progression. Additionally, cellular antioxidant activities like selenoamino acid metabolism and sulfur metabolism were also enriched in subgroup 2. Genes in subgroup 3 were enriched for autophagy regulation and epithelial mesenchymal transition (EMT). Upregulated genes in subgroup 5 were involved in angiogenesis.

Notably, we observed that subgroup 2 and 3 also involved in immune regulation. Specifically, subgroup 2 mainly participated in B cell and T cell signaling pathways, as well as interferon response, while subgroup 3 mostly involved in innate immune response including NOD-like and REG-I-like receptor signaling pathways.

Recently, accumulating studies have revealed essential roles of diabetes and insulin resistance in PDAC initiation and progression (*Zhang et al., 2019*; *Deng et al., 2022*). Interestingly, we also observed that gene functions in subgroup 1 and 2 were related to diabetes mellitus and insulin signaling pathway, which indicated their potential regulations in PDAC progression through mediating diabetes and insulin signaling pathways.

Taken together, these findings indicated that ductal cells in PDAC lesions consistently exhibited tumor malignancy patterns, while each subgroup executed its specific and diverse functions to fit together to mediate PDAC progression.

Gene expression patterns of malignant cells during PDAC progression

To further determine which subgroup in malignant cells is responsible for tumor initiation, pseudotime trajectory analysis was performed across them. Using R package monocle, the lineage differentiation trajectory was constructed as a tree-like structure (Fig. 4A, Fig. S6). Cells encountered four nodes and eight states during the trajectory progression: pre-branch (State 1, 2, 3, 8, 9) and the other two main progressive branches named branch 1 (State 4, 5, 6) and branch 2 (State 7) (Fig. 4B). Subgroup 4 and 5 mainly appeared at the beginning of the trajectory. Subgroup 2 predominantly appeared in the progressive state. Notably, there were several subgroups showing their abilities in transition. For instance, subgroup

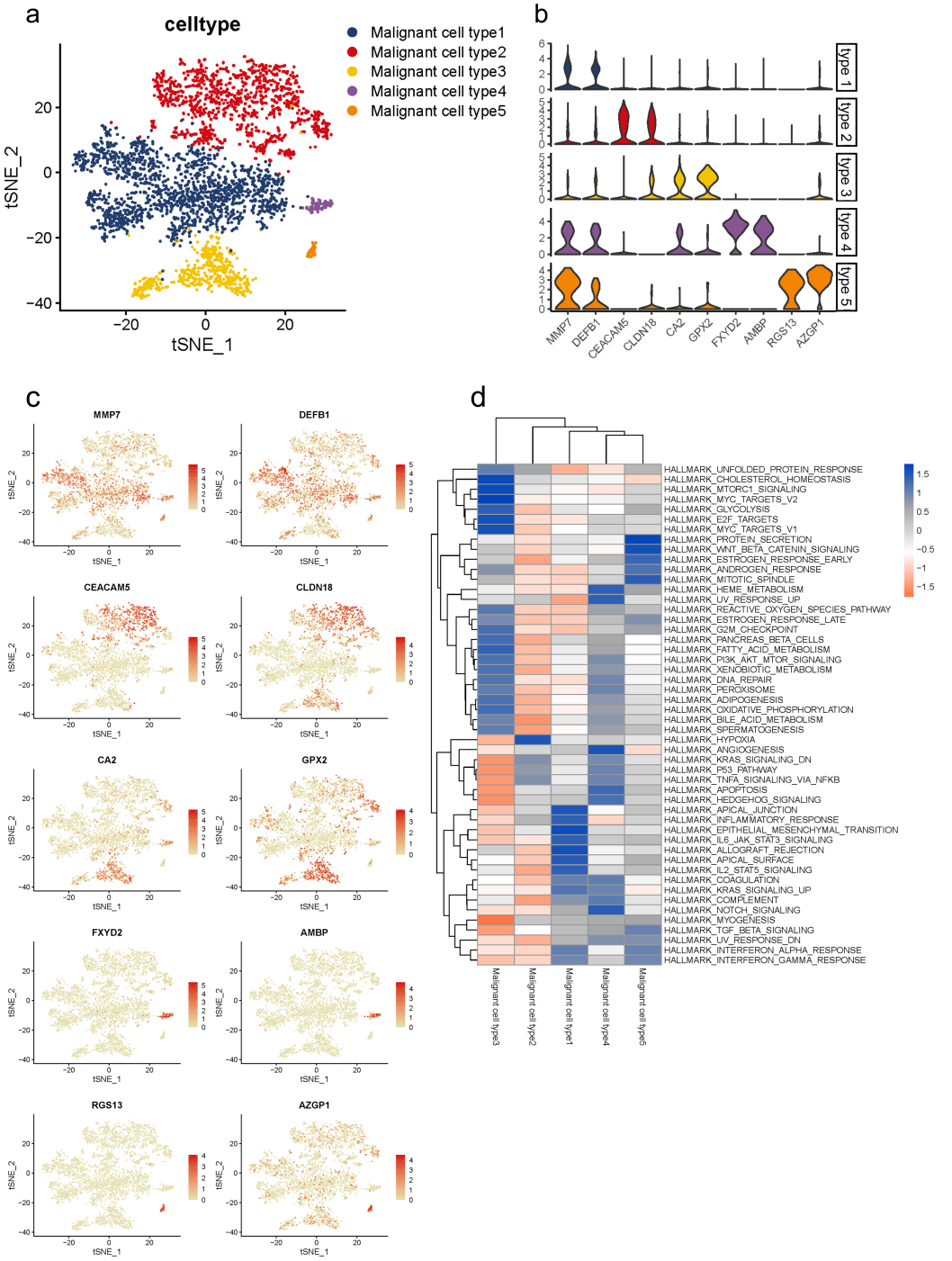

Figure 3 **Distinct subclusters of malignant ductal cells in primary PDAC lesions.** (A) a t-SNE plot showing five malignant ductal subclusters from 16 PDAC samples. (B) Violin plots for marker genes of each subcluster. (C) Feature plots for marker genes of each cluster. (D) Enrichment of Hallmark pathway terms in each subgroup.

Full-size DOI: 10.7717/peerj.17350/fig-3

1 and 3 mainly distributed throughout the beginning and branch 2, which showed a specific transitional direction from the beginning to branch 2. Subgroup 2 predominantly presented a specific transitional direction from the beginning to branch 1. Although these subgroups showed a preference in transition, they were detected at the terminal points of both branches, indicating their diverse forms along with the progression (Figs. 4C, 4D).

Along with the trajectory, cancer stem cell (CSC) marker ALDH1A1 persistently maintained a high level during transitions (*Lee, Dosch & Simeone, 2008*; *Sergeant et al., 2009*). During the transition to branch 1, cells sustained high expression levels of multiple reported poor prognosis PDAC markers like CEACAM5, HSPA6 and KLF4 (Fig. 4E) (*Deane & Brown, 2018*; *Gazzah et al., 2022*; *He, He & Xie, 2023*), which decreased during transition to branch 2. In addition, REG4, which is correlated with advanced stage, as well as one of the insulin-like growth factors, IGFBP3, both showed an upward trend in the transition to both branches (*Hwang et al., 2020*).

In addition, 5,633 genes whose expression significantly altered during transitions were analyzed (Table S4). In particular, a large portion of genes presenting malignant expression patterns was predominantly dysregulated along with the trajectory (Fig. 4F), including HMGA1, HMGB2, HES1, HIF1A, KLF2/4, ID1, FOS and P53, which were related to cell proliferation, EMT, DNA repair and hypoxia stress. Meanwhile, the alteration of multiple crucial oncogenic pathways (*Tempero et al., 2019*; *Yao, Maitra & Ying, 2020*), including Notch and PTEN signaling pathways, were remarkably activated. With featured gene expression patterns, we also found prominent changes in genes like CD55, HSP90AB1, REG4 and SPINK1 during the trajectory (Figs. 5A, 5B). Following the branched heatmap with BEAM analysis, genes were allocated to different clusters according to their expression features, and with the most divergent genes identified. These genes included S100A10, CEACAM5, NEAT1, MALAT1, SPINK1, REG4 and VEGFA (Fig. 5C).

Intercellular interactions in the TME

To better present a comprehensive and diverse landscape of interactions between malignant ductal cells and various stromal cells, we performed further subclustering of T cells and myeloid cells with known markers, since they are the major populations shaping immune landscape within the TME (*Ho, Jaffee & Zheng, 2020*). Specifically, T cells were subdivided into $CD4^+$ T cells (marked by CD4, SELL), $CD8^+$ T cytotoxic cells (marked by CD8, GZMB) and $CD8^+$ T exhausted cells (marked by CD8, TIGHT; Figs. S7A–S7C). Myeloid cells were subdivided into monocytes (marked by IL1B, FPR1), dendritic cells (marked by CLU, AREG) and macrophages (marked by CD163, CD86; Fig. S7D–S7F).

An analysis of the interactions between different cell types in the TME was generated by CellPhoneDB. Results of the intercellular ligand–receptor interactions could be visualized and analyzed through heatmap plots. It suggested that macrophages, $CD8^+$ T cells, monocytes and NK cells, had the largest number of interacting pairs and improved pairwise communications, consisting the core nodes of cell-to-cell interactions (Fig. S8). It was also determined that various cell types interacted extensively, which was based on broadcast ligand–receptor pairs we detected. (Figs. 6A, 6B).

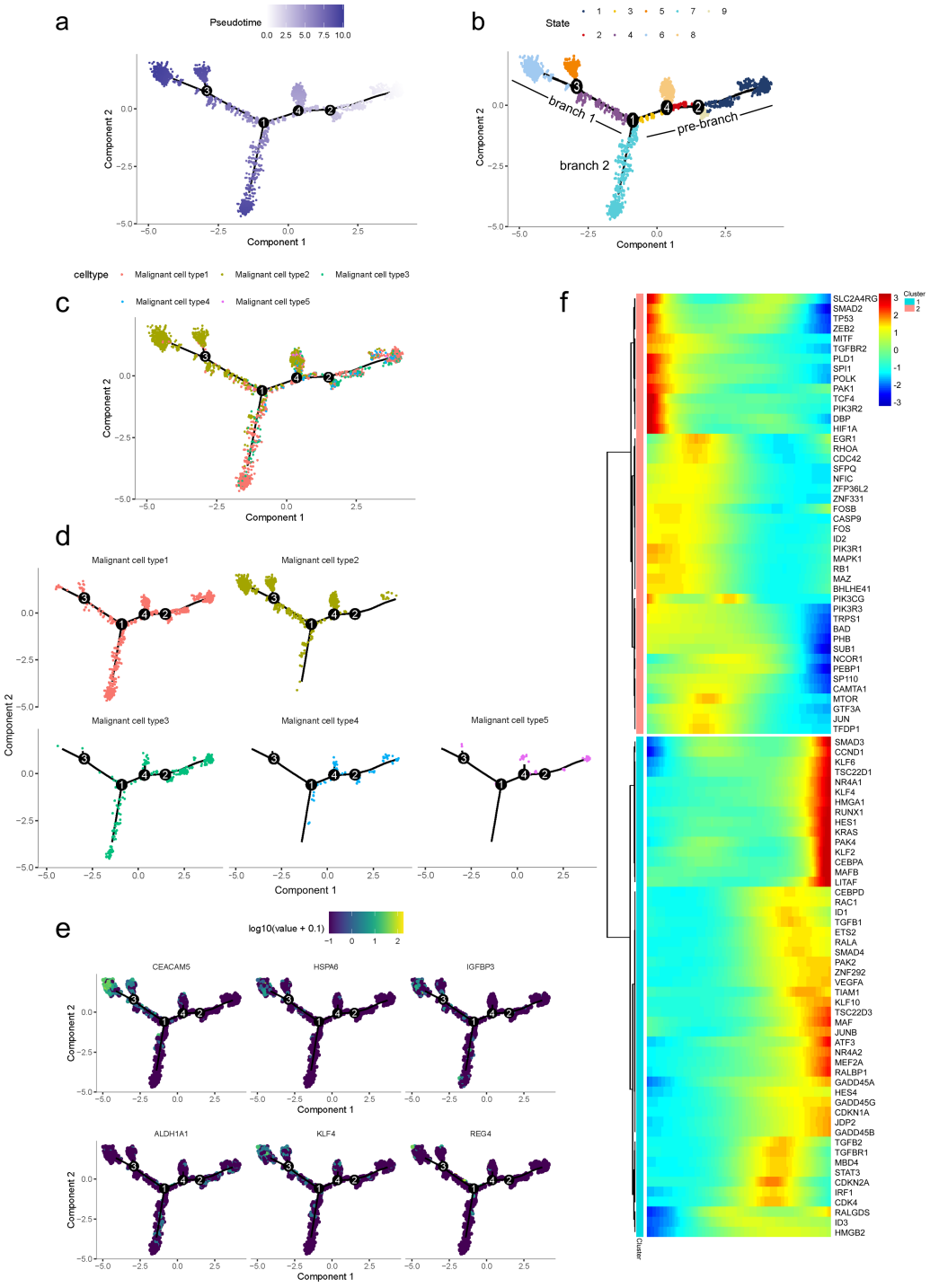

Figure 4 **Differential gene expression profiles along malignant progression.** (A) Pseudotime trajectory analysis of malignant ductal cells. (B) Cell states and branches, (C) distribution of five malignant subtypes and (D) distribution of each malignant subtype in pseudotime trajectory. (E) A single-cell trajectory plot showing expression of representative genes. (F) Expression of representative PDAC-associated genes across single cells depicted in a heatmap.

Full-size DOI: 10.7717/peerj.17350/fig-4

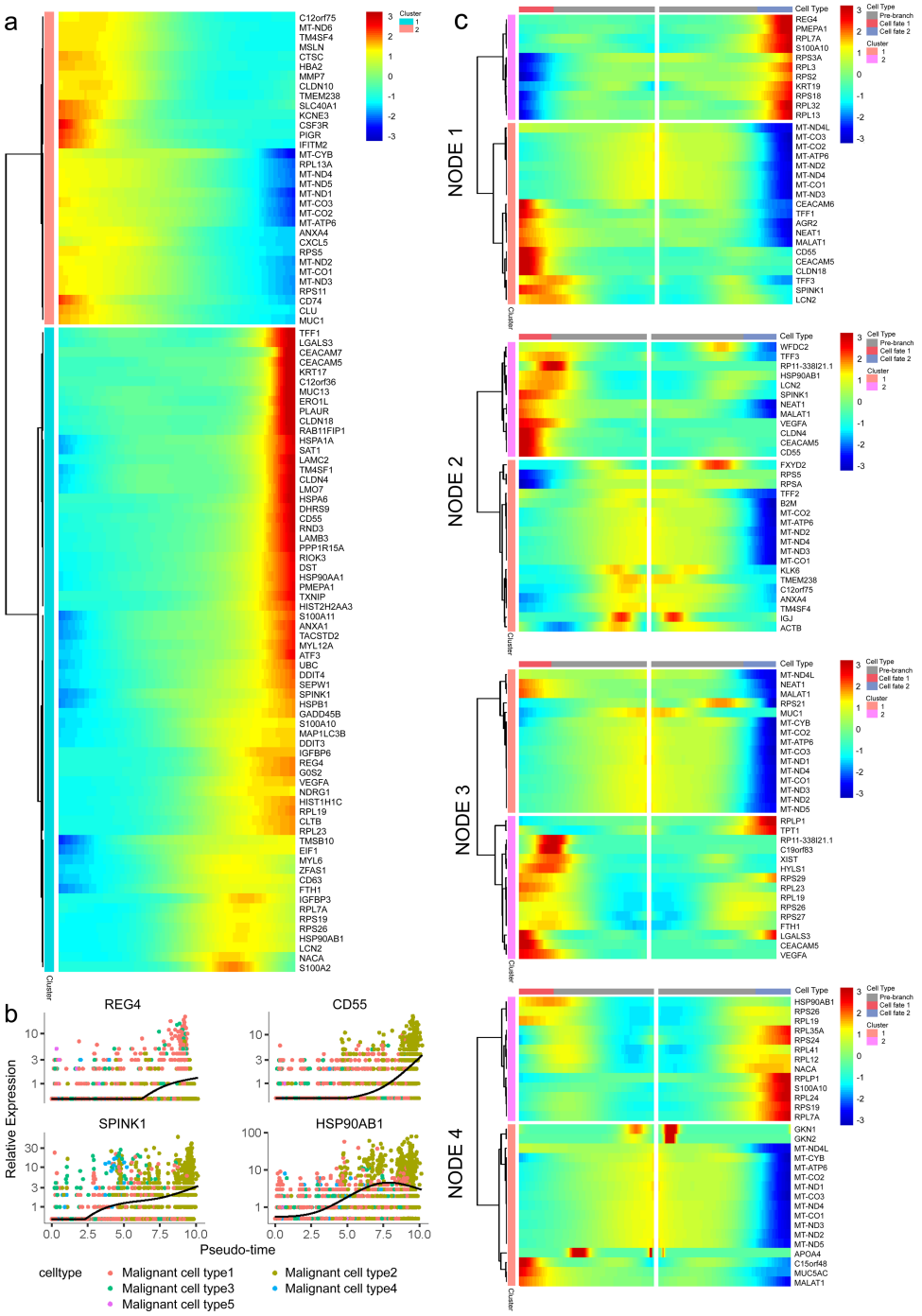

Figure 5 **Profiling of gene expression during progression of malignancies.** (A) A hierarchical heatmap clustering of DEGs following the pseudotime curve. (B) Representative expression patterns of genes during progression. (C) A pseudotime heatmap displaying DEGs between different branches based on the BEAM analysis.

Full-size DOI: 10.7717/peerj.17350/fig-5

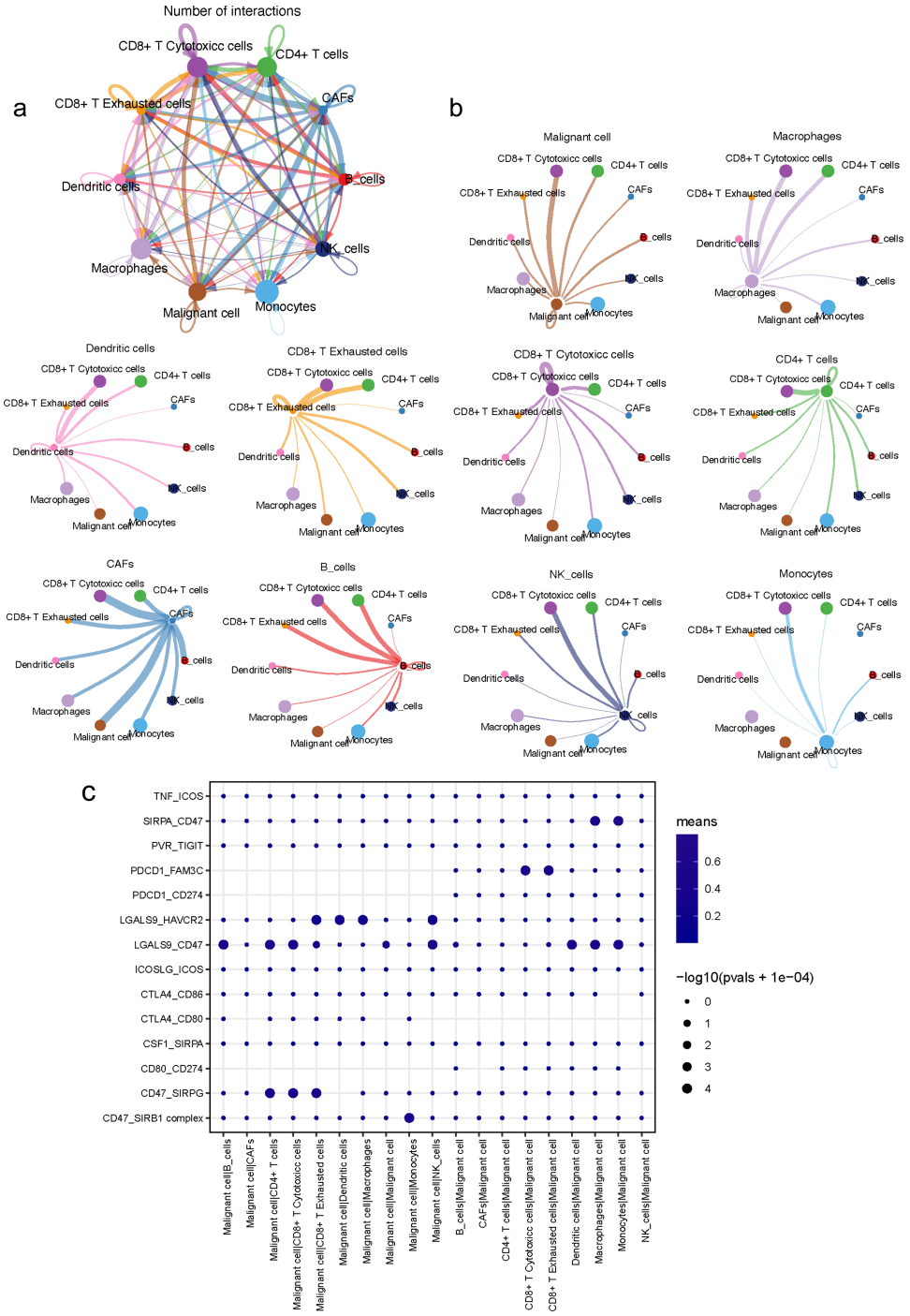

Figure 6 **Intensive crosstalk between malignant ductal cells and stromal cells in the TME.** (A) Intercellular crosstalk between malignant cells and stromal cells. (B) Detailed information regarding the ligands expressed by each subtype, as well as cells expressing cognate receptors. (C) A summary of selected ligand–receptor interactions in malignant cells under inhibitory interactions.

Full-size DOI: 10.7717/peerj.17350/fig-6

Meanwhile, an investigation of the inhibitory ligand–receptor complex between malignant ductal cells and other cell types was conducted. In addition to the well-defined inhibitory receptor–ligand pairs SIRPA-CD47, PVR-TIGHT and LGALS9-HAVCR2 (*Kučan Brlić et al., 2019*; *de Mingo Pulido et al., 2021*; *Jiang et al., 2021*), we found novel interactions between malignant cells and surrounding immune cells which were poorly investigated before, like PDCD1-FAM3C, LGALS9-CD47 and CSF1-SIRPA (Fig. 6C).

A wide range of costimulatory interactions, including known complexes like TNFRSF1A-GRN, MIF-TNFRSF14 and LGALS9-CD44, have also been discovered between malignant cells and other cell types (Fig. 7A). Interestingly, intensive interactions were found between macrophages and malignant cells, with four of the most commonly reported ligand–receptor pairs CD74-MIF, SPP1-CD44, CD74-COPA and CD74-APP, whose dysregulations are associated with tumor initiation and metastasis (*Stein et al., 2007*; *Orian-Rousseau, 2015*). These results indicated a pivotal role of macrophages through intensive functional interactions with other cells in PDAC progression, which is consistent with previous studies (*Vitale et al., 2019*). In addition, malignant cells also had common interactions with B cells, like CD74-COPA, CD74-MIF and CD74-APP. Meanwhile, we detected broad chemokine and receptor interactions between malignant cells and other cells (Fig. 7B), including CCR6-CCL20, CXCR3-CCL20 and CXCR6-CXCL16 (*Romero et al., 2020*), suggesting the chemoattraction potential of malignant ductal cells in the formation of a tumor-promoting microenvironment.

Validation of potential prognostic targets *in vitro*

Two potential prognostic genes, regenerating family member 4 (REG4) and serine peptidase inhibitor Kazal type 1 (SPINK1), were selected from DEG results aforementioned (Figs. 4 and 5). REG4 is known as a member of the calcium-dependent lectin gene superfamily, which aberrantly expresses in multiple cancers including PDAC (*Hwang et al., 2020*; *Bishnupuri et al., 2022*). SPINK1 is a protease inhibitor of trypsin in the pancreas, whose mutation usually relates to chronic pancreatitis (*Chen et al., 2018*; *Suzuki & Shimizu, 2019*; *Suwa et al., 2021*). These genes were reported to be closely related to PDAC malignant phenotypes by multiple studies, while mechanisms of which are still need to be further elucidated.

To investigate mRNA and protein levels of them, qRT-PCR and western blotting were performed on commonly used primary PDAC cell lines, BXPC-3, CAPAN-2 and MIA-PACA2, as well as a normal pancreatic ductal cell line HPNE as a control. We generally observed significant upregulated expressions in REG4 and SPINK1 at both mRNA and protein levels in all PDAC cell lines compared to HPNE (Figs. 8A, 8B). In addition, differentially expressed protein levels of them were observed by IHC staining of normal pancreas and PDAC tissues obtained from HPA database (Fig. S9). These results were consistent with our findings in scRNA-seq mentioned above.

Another important finding was the correlation between gene expression and immune infiltration in PDAC. TIMER analysis revealed that SPINK1 significantly correlated with a wide range of immune cell types (including $CD4^+$ T cells, $CD8^+$ T cells, macrophages, neutrophils and dendritic cells) and multiple immune inhibiting molecules (including

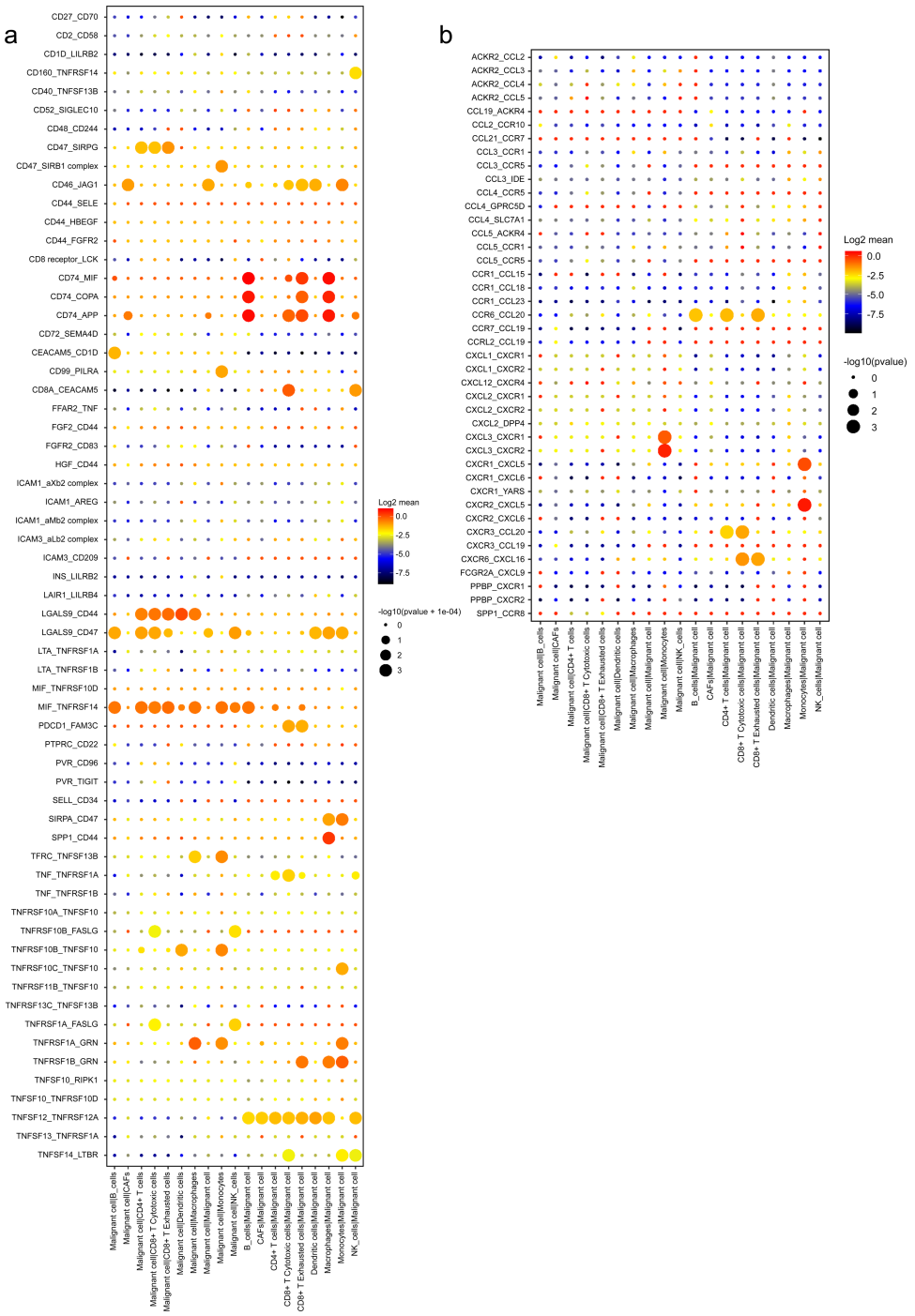

Figure 7 Stimulatory and chemokine interations between malignant ductal cells and other clusters. A summary of selected ligand–receptor interactions in malignant cells under (A) Stimulatory and (B) chemokine interactions.

Full-size DOI: 10.7717/peerj.17350/fig-7

CD274, CTLA4, PDCD1 and PDCD1LG2) (Fig. S10). In addition, it indicated that REG4 was almost an independent factor of immune infiltration. According to the Kaplan–Meier

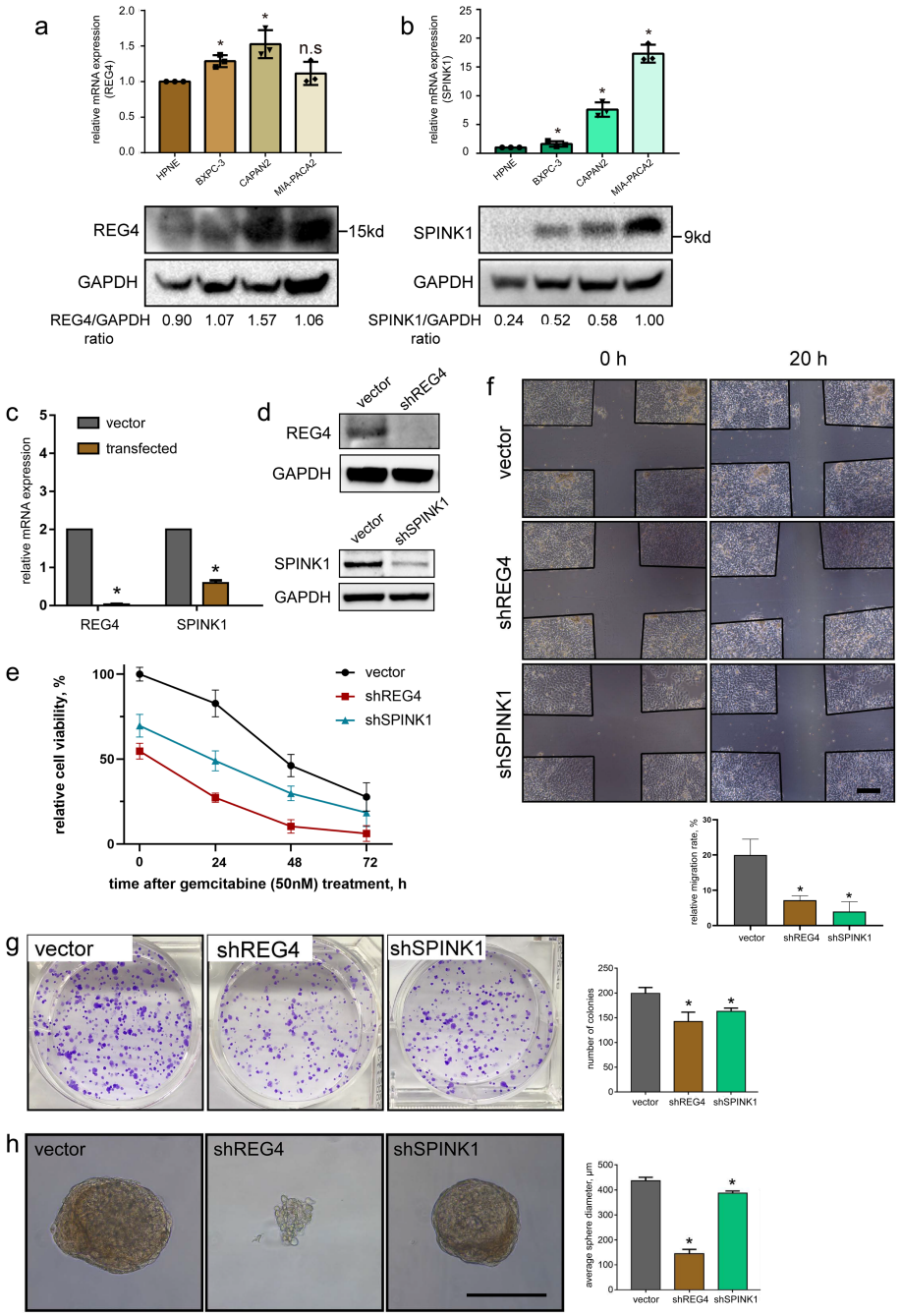

Figure 8 **Validation of gene expression and their potential effects on PDAC.** *In vitro* expression validation of potential prognostic genes. mRNA and protein expressions of (A) REG4 and (B) SPINK1 were obtained with qRT-PCR and western blotting assays respectively, with HPNE as a control. Transfection efficiency was validated by (C) mRNA and (D) protein levels. (E) Effects on MIA-PACA2 cell viability and its sensitivity to gemcitabine (50 nM) after genetical manipulation of 2 genes. A series of functional experiments including (F) wound healing, (G) colony formation and (H) sphere formation assays was conducted to examine the effect of REG4 and SPINK1. Scale bar = 500μm. $^{*}P < 0.05$ indicates statistical significance. n.s indicates non-significance.

Full-size DOI: 10.7717/peerj.17350/fig-8

analysis, a negative but nonsignificant correlation between overall survival rate of PDAC patients and gene expression of REG4 and SPINK1 was detected respectively (Fig. S11).

Further, stable transfected MIA-PACA2 cells were established to confirm potential effects of these two genes on PDAC progression (Figs. 8C, 8D). We found knockdown of REG4 or SPINK1 do alter a series of cancer-related characteristics in PDAC. In specific, MIA-PACA2 cells transfected with shREG4 or shSPINK1 exhibited significant decrease in proliferation, drug resistance, migration, invasion, as well as CSC features (Figs. 8E–8H).

DISCUSSION

PDAC is characterized by a high degree of intratumoral heterogeneity and aggressive features that constitutes the main obstacle to effective treatment (*Winter et al., 2012*; *Gobbi et al., 2013*; *Ryan, Hong & Bardeesy, 2014*; *Siegel et al., 2022*). Although profound achievements have been made for multiple solid tumors thanks to the advancement in single-cell technologies, it remains a challenging entity for studies in PDAC, due to the frequently low tumor cellularity and cellular heterogeneity in PDAC (*Kanda et al., 2012*; *Teng et al., 2015*; *Moffitt et al., 2015*; *Ho, Jaffee & Zheng, 2020*; *Steele et al., 2020*). There is no subtype that currently informs clinical decisions for PDAC yet (*Collisson et al., 2019*), so it is highly desirable to develop a *de novo* molecular taxonomy to guide treatment decisions.

Herein, we performed comprehensive analyses on a dataset of 16 primary PDAC lesions, accompanied with 3 adjacent tissues, at single-cell resolution, which revealed 6 major cell populations comprised of ductal cells and five stromal cellular types (myeloid cells, T cells, B cells, NK cells and CAFs). Malignant ductal cells were subclustered into five subpopulations with distinct transcriptomic and biological patterns, in line with previous results, highlighting substantial intratumoral heterogeneity in human primary PDACs (*Moffitt et al., 2015*; *Ho, Jaffee & Zheng, 2020*). Intensive crosstalk was found between malignant cell subtypes and stromal cells, which strongly overlaps with recent published PDAC scRNA-seq data (*Peng et al., 2019*; *Steele et al., 2020*; *Lee et al., 2021*). Meanwhile, we identified REG4 and SPINK1 as potential biomarkers for prognosis and therapeutic targets for PDAC.

Thanks to the development of novel transcriptomic techniques, especially single-cell sequencing, more different subtype classification schemes have been developed for PDAC, with majority agreement on a distinction between classical and basal-like phenotypes, which was originally proposed by Collisson and colleagues in 2011. The classical subtype usually presents well-differentiated subtypes of tumors characterized by epithelial gene expression, while mesenchymal genes are dominantly expressed in the basal-like tumor subtype (*Collisson et al., 2011*). The predominant discrepancy in metabolic features between classical and basal-like subtypes has been widely reported, with the classical subtype strongly associating with lipogenic phenotypes and the basal-like subtype preferentially wiring to glycolysis (*Daemen et al., 2015*; *Gutiérrez, Muñoz Bellvís & Orfao, 2021*). In addition, it has also been suggested that the basal-like subtype involves in a poorer prognosis and is less susceptible to chemotherapy compared with the classical subtype. As for our study, pathway analysis found known PDAC driver pathways, such as KRAS, MYC, MAPK

and WNT signaling pathways (*Australian Pancreatic Cancer Genome Initiative et al., 2012*; *Australian Pancreatic Cancer Genome Initiative et al., 2015*; *Witkiewicz et al., 2015*; *Raphael et al., 2017*), enriched in the five subtypes, which supported their tumor origin. Meanwhile, our results also correspond with the 'classical and basal-like' classification to a large extent. Specifically, we found representative pathways belonging to the classical subtype display specifically in subgroup 1 and 5, including steroid biosynthesis and cholesterol metabolism. While Subgroup 3 was predominantly enriched in hypoxia, KRAS signaling and EMT, sharing much more similarities with the basal-like features. Subgroup 2 presented a hybrid modality coexisting both classical (fatty acid metabolism and Notch pathway) and basal-like (glycolysis and KRAS signaling pathway) features. This result confirms recent notions that the molecular subtypes of PDAC cannot be directly recapitulated when it comes to individual cell populations analyzed at intratumoral levels (*Pompella et al., 2020*). In this regard, it is urgently necessary to identify PDAC exhibiting intermediate molecular features more precisely in order to reveal the great molecular heterogeneity of PDAC, as well as to exploit for therapies based on unique tumor subtypes. It also highlights the need to include an expanded cohort for further studies to make a firm conclusion.

It has been generally accepted that an elevated insulin level (hyperinsulinemia) indicates a common phenomenon in PDAC patients and a signal for poor clinical outcomes (*Zhang et al., 2019*; *Deng et al., 2022*). Insulin triggers signaling cascades implicated in tumorigenesis that promotes mitogenic activities (*Pollak, 2008*). Meanwhile, relevant researches indicated that insulin restored the capacity to instigate invasion and proliferation in pancreatic ductal cells with the introduction of KRAS mutation (*Boursi et al., 2017*; *Carreras-Torres et al., 2017*). While the failure in clinical trials aimed at insulin and relevant signaling pathways indicates that mechanisms by which insulin influences PDAC development are still unclear (*Zhang et al., 2019*). Notably, our study has strengthened the insulin-cancer notion by revealing functional enrichment in diabetes mellitus and insulin signaling pathways for subtype 1 and 2. Extensive explorations focused on insulin signaling pathways are needed to find novel druggable targets for PDAC therapy.

PDAC microenvironment is highly immunosuppressive, featured by a dense desmoplastic stroma that interferes with blood flow, inhibits drug delivery, and suppresses antitumor immunity (*Looi et al., 2019*; *Ho, Jaffee & Zheng, 2020*). Notably, unique immune-related signatures including TNF-β signaling and EMT were detected in subgroup 3 that could be distinguished from other subtypes in our study. On the one side, TGF-β blockage and EMT inhibition have been shown to reprogram the TME context and modify its immunologic conditions (*Gough, Xiang & Mishra, 2021*). On the other side, subgroup 2 and 3 also functioned extensively in immune regulation, involving various innate immune responses and immune cells including B cells, T cells and NK cells, which further contributed to immune escape of tumor cells.

Moreover, intimate cell–cell interactions among malignant cells and other stromal cells were suggested in our study as previously reported (*Wang et al., 2021*). It is possible that the resistance to tumor immunotherapy might be attributed to high levels of inhibitory receptor–ligand complexes (*Jiang et al., 2021*). Additionally, upregulated chemokine expressions, like CCL5 and CCL20 (*Romero et al., 2020*), might facilitate immune cells

recruited to tumors. Macrophages interacted most intensively with other cells (*Vitale et al., 2019*), suggesting their potential and promising abilities in anti-tumor treatments. Several studies have illustrated that CSCs are the primary source of tumorigenesis (*Peng et al., 2019*; *Nimmakayala et al., 2021*). As for our trajectory analysis, we found known CSC makers, such as ALDH1A1 (*Lee, Dosch & Simeone, 2008*; *Sergeant et al., 2009*), altered significantly during the transition to the malignant phenotype as well. Meanwhile, REG4 (*Hwang et al., 2020*) and SPINK1 (*Suzuki & Shimizu, 2019*), two of the potential differentially expressed genes validated to significantly upregulate during the trajectory, have been suggested to act as factors promoting CSC properties, which were also validated by sphere formation assay in our study (Fig. 8H). Moreover, we were intrigued to find impacts of both REG4 and SPINK1 on cell proliferation, drug resistance, migration and invasion abilities through functional validation assays. This finding suggests potential pivotal roles for REG4 and SPINK1 in PDAC progression and they may hold promise as potential therapeutic targets for PDAC in the future. We also found that multiple canonical oncogenic pathways, such as Notch and PTEN signaling pathways, were activated during trajectory progression. Based on our result, these pathways may be implicated in key molecular regulations in PDAC progression. However, these results in our analysis need more confirmation in future studies.

CONCLUSIONS

Our understanding of the ductal cell subpopulations in PDAC offers new insights into evolving a novel framework for metabolic and immunologic therapies. REG4 and SPINK1 are expected to be promising prognostic markers for PDAC therapy. Further researches are needed to uncover the molecular mechanisms.

ACKNOWLEDGEMENTS

We would like to give our sincere appreciation to the reviewers for their helpful comments on this article and the research group for the NCBI, which provided data for this collection.

ADDITIONAL INFORMATION AND DECLARATIONS

Funding

This work was supported by National Natural Science Foundation of China (No. 82072650) and the Natural Science Foundation of Zhejiang province, China (No. LQ21H160037). The funders had no role in study design, data collection and analysis, decision to publish, or preparation of the manuscript.

Grant Disclosures

The following grant information was disclosed by the authors:
National Natural Science Foundation of China: 82072650.
Natural Science Foundation of Zhejiang province, China: LQ21H160037.

Competing Interests

The authors declare there are no competing interests.

Author Contributions

- Yutian Ji conceived and designed the experiments, performed the experiments, analyzed the data, prepared figures and/or tables, authored or reviewed drafts of the article, and approved the final draft.
- Qianhui Xu performed the experiments, analyzed the data, prepared figures and/or tables, and approved the final draft.
- Weilin Wang conceived and designed the experiments, authored or reviewed drafts of the article, and approved the final draft.

Data Availability

The following information was supplied regarding data availability:

The datasets analyzed for this study is available at GEO: GSE155698.

The original blots, codes for analysis and the qRT-PCR results are available in the Supplementary Files.

Supplemental Information

Supplemental information for this article can be found online at http://dx.doi.org/10.7717/peerj.17350#supplemental-information.

REFERENCES

Australian Pancreatic Cancer Genome Initiative, Biankin AV, Waddell N, Kassahn KS, Gingras M-C, Muthuswamy LB, Johns AL, Miller DK, Wilson PJ, Patch A-M, Wu J, Chang DK, Cowley MJ, Gardiner BB, Song S, Harliwong I, Idrisoglu S, Nourse C, Nourbakhsh E, Manning S, Wani S, Gongora M, Pajic M, Scarlett CJ, Gill AJ, Pinho AV, Rooman I, Anderson M, Holmes O, Leonard C, Taylor D, Wood S, Xu Q, Nones K, Lynn Fink J, Christ A, Bruxner T, Cloonan N, Kolle G, Newell F, Pinese M, Scott Mead R, Humphris JL, Kaplan W, Jones MD, Colvin EK, Nagrial AM, Humphrey ES, Chou A, Chin VT, Chantrill LA, Mawson A, Samra JS, Kench JG, Lovell JA, Daly RJ, Merrett ND, Toon C, Epari K, Nguyen NQ, Barbour A, Zeps N, Kakkar N, Zhao F, Qing Wu Y, Wang M, Muzny DM, Fisher WE, Charles Brunicardi F, Hodges SE, Reid JG, Drummond J, Chang K, Han Y, Lewis LR, Dinh H, Buhay CJ, Beck T, Timms L, Sam M, Begley K, Brown A, Pai D, Panchal A, Buchner N, De Borja R, Denroche RE, Yung CK, Serra S, Onetto N, Mukhopadhyay D, Tsao M-S, Shaw PA, Petersen GM, Gallinger S, Hruban RH, Maitra A, Iacobuzio-Donahue CA, Schulick RD, Wolfgang CL, Morgan RA, Lawlor RT, Capelli P, Corbo V, Scardoni M, Tortora G, Tempero MA, Mann KM, Jenkins NA, Perez-Mancera PA, Adams DJ, Largaespada DA, Wessels LFA, Rust AG, Stein LD, Tuveson DA, Copeland NG, Musgrove EA, Scarpa A, Eshleman JR, Hudson TJ, Sutherland RL, Wheeler DA, Pearson JV, McPherson JD, Gibbs RA, Grimmond SM. 2012. Pancreatic cancer genomes reveal aberrations in axon guidance pathway genes. *Nature* **491**:399–405 DOI 10.1038/nature11547.

Australian Pancreatic Cancer Genome Initiative, Waddell N, Pajic M, Patch A-M, Chang DK, Kassahn KS, Bailey P, Johns AL, Miller D, Nones K, Quek K, Quinn MCJ, Robertson AJ, Fadlullah MZH, Bruxner TJC, Christ AN, Harliwong I, Idrisoglu S, Manning S, Nourse C, Nourbakhsh E, Wani S, Wilson PJ, Markham E, Cloonan N, Anderson MJ, Fink JL, Holmes O, Kazakoff SH, Leonard C, Newell F, Poudel B, Song S, Taylor D, Waddell N, Wood S, Xu Q, Wu J, Pinese M, Cowley MJ, Lee HC, Jones MD, Nagrial AM, Humphris J, Chantrill LA, Chin V, Steinmann AM, Mawson A, Humphrey ES, Colvin EK, Chou A, Scarlett CJ, Pinho AV, Giry-Laterriere M, Rooman I, Samra JS, Kench JG, Pettitt JA, Merrett ND, Toon C, Epari K, Nguyen NQ, Barbour A, Zeps N, Jamieson NB, Graham JS, Niclou SP, Bjerkvig R, Grützmann R, Aust D, Hruban RH, Maitra A, Iacobuzio-Donahue CA, Wolfgang CL, Morgan RA, Lawlor RT, Corbo V, Bassi C, Falconi M, Zamboni G, Tortora G, Tempero MA, Gill AJ, Eshleman JR, Pilarsky C, Scarpa A, Musgrove EA, Pearson JV, Biankin AV, Grimmond SM. 2015. Whole genomes redefine the mutational landscape of pancreatic cancer. *Nature* **518**:495–501 DOI 10.1038/nature14169.

Bishnupuri KS, Sainathan SK, Ciorba MA, Houchen CW, Dieckgraefe BK. 2022. Reg4 interacts with CD44 to regulate proliferation and stemness of colorectal and pancreatic cancer cells. *Molecular Cancer Research* **20**:387–399 DOI 10.1158/1541-7786.MCR-21-0224.

Boursi B, Finkelman B, Giantonio BJ, Haynes K, Rustgi AK, Rhim AD, Mamtani R, Yang Y-X. 2017. A clinical prediction model to assess risk for pancreatic cancer among patients with new-onset diabetes. *Gastroenterology* **152**:840–850 DOI 10.1053/j.gastro.2016.11.046.

Carreras-Torres R, Johansson M, Gaborieau V, Haycock PC, Wade KH, Relton CL, Martin RM, Davey Smith G, Brennan P. 2017. The role of obesity, type 2 diabetes, and metabolic factors in pancreatic cancer: a Mendelian randomization study. *JNCI: Journal of the National Cancer Institute* **109**:djx012 DOI 10.1093/jnci/djx012.

Chen F, Long Q, Fu D, Zhu D, Ji Y, Han L, Zhang B, Xu Q, Liu B, Li Y, Wu S, Yang C, Qian M, Xu J, Liu S, Cao L, Chin YE, Lam EW-F, Coppé J-P, Sun Y. 2018. Targeting SPINK1 in the damaged tumour microenvironment alleviates therapeutic resistance. *Nature Communications* **9**:4315 DOI 10.1038/s41467-018-06860-4.

Collisson EA, Bailey P, Chang DK, Biankin AV. 2019. Molecular subtypes of pancreatic cancer. *Nature Reviews Gastroenterology & Hepatology* **16**:207–220 DOI 10.1038/s41575-019-0109-y.

Collisson EA, Sadanandam A, Olson P, Gibb WJ, Truitt M, Gu S, Cooc J, Weinkle J, Kim GE, Jakkula L, Feiler HS, Ko AH, Olshen AB, Danenberg KL, Tempero MA, Spellman PT, Hanahan D, Gray JW. 2011. Subtypes of pancreatic ductal adenocarcinoma and their differing responses to therapy. *Nature Medicine* **17**:500–503 DOI 10.1038/nm.2344.

Cui D, Dai X, Shu J, Ma Y, Wei D, Xiong X, Zhao Y. 2020. The cross talk of two family members of β-TrCP in the regulation of cell autophagy and growth. *Cell Death & Differentiation* **27**:1119–1133 DOI 10.1038/s41418-019-0402-x.

Daemen A, Peterson D, Sahu N, McCord R, Du X, Liu B, Kowanetz K, Hong R, Moffat J, Gao M, Boudreau A, Mroue R, Corson L, O'Brien T, Qing J, Sampath D, Merchant M, Yauch R, Manning G, Settleman J, Hatzivassiliou G, Evangelista M. 2015. Metabolite profiling stratifies pancreatic ductal adenocarcinomas into subtypes with distinct sensitivities to metabolic inhibitors. *Proceedings of the National Academy of Sciences of the United States of America* **112**:E4410-E4417 DOI 10.1073/pnas.1501605112.

de Mingo Pulido Á, Hänggi K, Celias DP, Gardner A, Li J, Batista-Bittencourt B, Mohamed E, Trillo-Tinoco J, Osunmakinde O, Peña R, Onimus A, Kaisho T, Kaufmann J, McEachern K, Soliman H, Luca VC, Rodriguez PC, Yu X, Ruffell B. 2021. The inhibitory receptor TIM-3 limits activation of the cGAS-STING pathway in intra-tumoral dendritic cells by suppressing extracellular DNA uptake. *Immunity* **54**:1154–1167 DOI 10.1016/j.immuni.2021.04.019.

Deane CAS, Brown IR. 2018. Knockdown of Heat Shock Proteins HSPA6 (Hsp70B') and HSPA1A (Hsp70-1) sensitizes differentiated human neuronal cells to cellular stress. *Neurochemical Research* **43**:340–350 DOI 10.1007/s11064-017-2429-z.

Deng J, Guo Y, Du J, Gu J, Kong L, Tao B, Li J, Fu D. 2022. The intricate crosstalk between insulin and pancreatic ductal adenocarcinoma: a review from clinical to molecular. *Frontiers in Cell and Developmental Biology* **10**:844028 DOI 10.3389/fcell.2022.844028.

Efremova M, Vento-Tormo M, Teichmann SA, Vento-Tormo R. 2020. CellPhoneDB: inferring cell–cell communication from combined expression of multi-subunit ligand–receptor complexes. *Nature Protocols* **15**:1484–1506 DOI 10.1038/s41596-020-0292-x.

Elyada E, Bolisetty M, Laise P, Flynn WF, Courtois ET, Burkhart RA, Teinor JA, Belleau P, Biffi G, Lucito MS, Sivajothi S, Armstrong TD, Engle DD, Yu KH, Hao Y, Wolfgang CL, Park Y, Preall J, Jaffee EM, Califano A, Robson P, Tuveson DA. 2019. Cross-species single-cell analysis of pancreatic ductal adenocarcinoma reveals antigen-presenting cancer-associated fibroblasts. *Cancer Discovery* **9**:1102–1123 DOI 10.1158/2159-8290.CD-19-0094.

Gazzah A, Bedard PL, Hierro C, Kang Y-K, Abdul Razak A, Ryu M-H, Demers B, Fagniez N, Henry C, Hospitel M, Soria J-C, Tabernero J. 2022. Safety, pharmacokinetics, and antitumor activity of the anti-CEACAM5-DM4 antibody-drug conjugate tusamitamab ravtansine (SAR408701) in patients with advanced solid tumors: first-in-human dose-escalation study. *Annals of Oncology* **33**:416–425 DOI 10.1016/j.annonc.2021.12.012.

Gobbi PG, Bergonzi M, Comelli M, Villano L, Pozzoli D, Vanoli A, Dionigi P. 2013. The prognostic role of time to diagnosis and presenting symptoms in patients with pancreatic cancer. *Cancer Epidemiology* **37**:186–190 DOI 10.1016/j.canep.2012.12.002.

Gough NR, Xiang X, Mishra L. 2021. TGF- β signaling in liver, pancreas, and gastrointestinal diseases and cancer. *Gastroenterology* **161**:434–452 DOI 10.1053/j.gastro.2021.04.064.

Gutiérrez ML, Muñoz Bellvís L, Orfao A. 2021. Genomic heterogeneity of pancreatic ductal adenocarcinoma and its clinical impact. *Cancers* **13**:4451 DOI 10.3390/cancers13174451.

Hänzelmann S, Castelo R, Guinney J. 2013. GSVA: gene set variation analysis for microarray and RNA-Seq data. *BMC Bioinformatics* **14**:7 DOI 10.1186/1471-2105-14-7.

He Z, He J, Xie K. 2023. KLF4 transcription factor in tumorigenesis. *Cell Death Discovery* **9**:118 DOI 10.1038/s41420-023-01416-y.

Heining C, Horak P, Uhrig S, Codo PL, Klink B, Hutter B, Fröhlich M, Bonekamp D, Richter D, Steiger K, Penzel R, Endris V, Ehrenberg KR, Frank S, Kleinheinz K, Toprak UH, Schlesner M, Mandal R, Schulz L, Lambertz H, Fetscher S, Bitzer M, Malek NP, Horger M, Giese NA, Strobel O, Hackert T, Springfeld C, Feuerbach L, Bergmann F, Schröck E, von Kalle C, Weichert W, Scholl C, Ball CR, Stenzinger A, Brors B, Fröhling S, Glimm H. 2018. NRG1 fusions in *KRAS* wild-type pancreatic cancer. *Cancer Discovery* **8**:1087–1095 DOI 10.1158/2159-8290.CD-18-0036.

Hezel AF, Kimmelman AC, Stanger BZ, Bardeesy N, De Pinho RA. 2006. Genetics and biology of pancreatic ductal adenocarcinoma. *Genes & Development* **20**:1218–1249 DOI 10.1101/gad.1415606.

Ho WJ, Jaffee EM, Zheng L. 2020. The tumour microenvironment in pancreatic cancer —clinical challenges and opportunities. *Nature Reviews Clinical Oncology* **17**:527–540 DOI 10.1038/s41571-020-0363-5.

Honeder S, Tomin T, Nebel L, Gindlhuber J, Fritz-Wallace K, Schinagl M, Heininger C, Schittmayer M, Ghaffari-Tabrizi-Wizsy N, Birner-Gruenberger R. 2021. Adipose triglyceride lipase loss promotes a metabolic switch in A549 non–small cell lung cancer cell spheroids. *Molecular & Cellular Proteomics* **20**:100095 DOI 10.1016/j.mcpro.2021.100095.

Hosein AN, Dougan SK, Aguirre AJ, Maitra A. 2022. Translational advances in pancreatic ductal adenocarcinoma therapy. *Nature Cancer* **3**:272–286 DOI 10.1038/s43018-022-00349-2.

Hosein AN, Huang H, Wang Z, Parmar K, Du W, Huang J, Maitra A, Olson E, Verma U, Brekken RA. 2019. Cellular heterogeneity during mouse pancreatic ductal adenocarcinoma progression at single-cell resolution. *JCI Insight* **4**:e129212 DOI 10.1172/jci.insight.129212.

Hwang J, Yoon J, Cho Y, Cha P, Park J, Choi K. 2020. A mutant KRAS-induced factor REG4 promotes cancer stem cell properties *via* Wnt/ β-catenin signaling. *International Journal of Cancer* **146**:2877–2890 DOI 10.1002/ijc.32728.

Jiang Z, Sun H, Yu J, Tian W, Song Y. 2021. Targeting CD47 for cancer immunotherapy. *Journal of Hematology & Oncology* **14**:180 DOI 10.1186/s13045-021-01197-w.

Kanda M, Matthaei H, Wu J, Hong S, Yu J, Borges M, Hruban RH, Maitra A, Kinzler K, Vogelstein B, Goggins M. 2012. Presence of somatic mutations in most early-stage pancreatic intraepithelial neoplasia. *Gastroenterology* **142**:730–733 DOI 10.1053/j.gastro.2011.12.042.

Karasinska JM, Topham JT, Kalloger SE, Jang GH, Denroche RE, Culibrk L, Williamson LM, Wong H-L, Lee MKC, O'Kane GM, Moore RA, Mungall AJ, Moore MJ, Warren C, Metcalfe A, Notta F, Knox JJ, Gallinger S, Laskin J, Marra MA, Jones SJM, Renouf DJ, Schaeffer DF. 2020. Altered gene expression along the glycolysis–cholesterol synthesis axis is associated with outcome in pancreatic cancer. *Clinical Cancer Research* **26**:135–146 DOI 10.1158/1078-0432.CCR-19-1543.

Katz MHG, Shi Q, Meyers JP, Herman JM, Choung M, Wolpin BM, Ahmad S, Marsh R de W, Schwartz LH, Behr S, Frankel WL, Collisson EA, Leenstra JL, Williams TM, Vaccaro GM, Venook AP, Meyerhardt JA, O'Reilly EM. 2021. Alliance A021501: preoperative mFOLFIRINOX or mFOLFIRINOX plus hypofractionated radiation therapy (RT) for borderline resectable (BR) adenocarcinoma of the pancreas. *Journal of Clinical Oncology* **39**:377–377 DOI 10.1200/JCO.2021.39.3_suppl.377.

Kučan Brlić P, Lenac Roviš T, Cinamon G, Tsukerman P, Mandelboim O, Jonjić S. 2019. Targeting PVR (CD155) and its receptors in anti-tumor therapy. *Cellular & Molecular Immunology* **16**:40–52 DOI 10.1038/s41423-018-0168-y.

Lee CJ, Dosch J, Simeone DM. 2008. Pancreatic cancer stem cells. *Journal of Clinical Oncology* **26**:2806–2812 DOI 10.1200/JCO.2008.16.6702.

Lee JJ, Bernard V, Semaan A, Monberg ME, Huang J, Stephens BM, Lin D, Rajapakshe KI, Weston BR, Bhutani MS, Haymaker CL, Bernatchez C, Taniguchi CM, Maitra A, Guerrero PA. 2021. Elucidation of tumor-stromal heterogeneity and the ligand-receptor interactome by single-cell transcriptomics in real-world pancreatic cancer biopsies. *Clinical Cancer Research* **27**:5912–5921 DOI 10.1158/1078-0432.CCR-20-3925.

Li B, Severson E, Pignon J-C, Zhao H, Li T, Novak J, Jiang P, Shen H, Aster JC, Rodig S, Signoretti S, Liu JS, Liu XS. 2016. Comprehensive analyses of tumor immunity: implications for cancer immunotherapy. *Genome Biology* **17**:174 DOI 10.1186/s13059-016-1028-7.

Li L, Dong J, Yan L, Yong J, Liu X, Hu Y, Fan X, Wu X, Guo H, Wang X, Zhu X, Li R, Yan J, Wei Y, Zhao Y, Wang W, Ren Y, Yuan P, Yan Z, Hu B, Guo F, Wen L, Tang F, Qiao J. 2017. Single-cell RNA-Seq analysis maps development of human germline cells and gonadal niche interactions. *Cell Stem Cell* **20**:858–873 DOI 10.1016/j.stem.2017.03.007.

Liberzon A, Subramanian A, Pinchback R, Thorvaldsdóttir H, Tamayo P, Mesirov JP. 2011. Molecular signatures database (MSigDB) 3.0. *Bioinformatics* **27**:1739–1740 DOI 10.1093/bioinformatics/btr260.

Ligorio M, Sil S, Malagon-Lopez J, Nieman LT, Misale S, Di Pilato M, Ebright RY, Karabacak MN, Kulkarni AS, Liu A, Vincent Jordan N, Franses JW, Philipp J, Kreuzer J, Desai N, Arora KS, Rajurkar M, Horwitz E, Neyaz A, Tai E, Magnus NKC, Vo KD, Yashaswini CN, Marangoni F, Boukhali M, Fatherree JP, Damon LJ, Xega K, Desai R, Choz M, Bersani F, Langenbucher A, Thapar V, Morris R, Wellner UF, Schilling O, Lawrence MS, Liss AS, Rivera MN, Deshpande V, Benes CH, Maheswaran S, Haber DA, Fernandez-Del-Castillo C, Ferrone CR, Haas W,

Aryee MJ, Ting DT. 2019. Stromal Microenvironment Shapes the Intratumoral Architecture of Pancreatic Cancer. *Cell* **178**:160–175 DOI 10.1016/j.cell.2019.05.012.

Lin W, Noel P, Borazanci EH, Lee J, Amini A, Han IW, Heo JS, Jameson GS, Fraser C, Steinbach M, Woo Y, Fong Y, Cridebring D, Von Hoff DD, Park JO, Han H. 2020. Single-cell transcriptome analysis of tumor and stromal compartments of pancreatic ductal adenocarcinoma primary tumors and metastatic lesions. *Genome Medicine* **12**:80 DOI 10.1186/s13073-020-00776-9.

Looi C-K, Chung FF-L, Leong C-O, Wong S-F, Rosli R, Mai C-W. 2019. Therapeutic challenges and current immunomodulatory strategies in targeting the immunosuppressive pancreatic tumor microenvironment. *Journal of Experimental & Clinical Cancer Research* **38**:162 DOI 10.1186/s13046-019-1153-8.

Moffitt RA, Marayati R, Flate EL, Volmar KE, Loeza SGH, Hoadley KA, Rashid NU, Williams LA, Eaton SC, Chung AH, Smyla JK, Anderson JM, Kim HJ, Bentrem DJ, Talamonti MS, Iacobuzio-Donahue CA, Hollingsworth MA, Yeh JJ. 2015. Virtual microdissection identifies distinct tumor- and stroma-specific subtypes of pancreatic ductal adenocarcinoma. *Nature Genetics* **47**:1168–1178 DOI 10.1038/ng.3398.

Nimmakayala RK, Leon F, Rachagani S, Rauth S, Nallasamy P, Marimuthu S, Shailendra GK, Chhonker YS, Chugh S, Chirravuri R, Gupta R, Mallya K, Prajapati DR, Lele SM, Caffrey CT, Grem LJ, Grandgenett PM, Hollingsworth MA, Murry DJ, Batra SK, Ponnusamy MP. 2021. Metabolic programming of distinct cancer stem cells promotes metastasis of pancreatic ductal adenocarcinoma. *Oncogene* **40**:215–231 DOI 10.1038/s41388-020-01518-2.

Oettle H, Neuhaus P, Hochhaus A, Hartmann JT, Gellert K, Ridwelski K, Niedergethmann M, Zülke C, Fahlke J, Arning MB, Sinn M, Hinke A, Riess H. 2013. Adjuvant chemotherapy with gemcitabine and long-term outcomes among patients with resected pancreatic cancer: the CONKO-001 randomized trial. *JAMA* **310**:1473 DOI 10.1001/jama.2013.279201.

Orian-Rousseau V. 2015. CD44 acts as a signaling platform controlling tumor progression and metastasis. *Frontiers in Immunology* **6**:154 DOI 10.3389/fimmu.2015.00154.

Patel AP, Tirosh I, Trombetta JJ, Shalek AK, Gillespie SM, Wakimoto H, Cahill DP, Nahed BV, Curry WT, Martuza RL, Louis DN, Rozenblatt-Rosen O, Suvà ML, Regev A, Bernstein BE. 2014. Single-cell RNA-seq highlights intratumoral heterogeneity in primary glioblastoma. *Science* **344**:1396–1401 DOI 10.1126/science.1254257.

Peng J, Sun B-F, Chen C-Y, Zhou J-Y, Chen Y-S, Chen H, Liu L, Huang D, Jiang J, Cui G-S, Yang Y, Wang W, Guo D, Dai M, Guo J, Zhang T, Liao Q, Liu Y, Zhao Y-L, Han D-L, Zhao Y, Yang Y-G, Wu W. 2019. Single-cell RNA-seq highlights intra-tumoral heterogeneity and malignant progression in pancreatic ductal adenocarcinoma. *Cell Research* **29**:725–738 DOI 10.1038/s41422-019-0195-y.

Pollak M. 2008. Insulin and insulin-like growth factor signalling in neoplasia. *Nature Reviews Cancer* **8**:915–928 DOI 10.1038/nrc2536.

Pompella L, Tirino G, Pappalardo A, Caterino M, Ventriglia A, Nacca V, Orditura M, Ciardiello F, De Vita F. 2020. Pancreatic cancer molecular classifications: from bulk

genomics to single cell analysis. *International Journal of Molecular Sciences* **21**:2814 DOI 10.3390/ijms21082814.

Raphael BJ, Hruban RH, Aguirre AJ, Moffitt RA, Yeh JJ, Stewart C, Robertson AG, Cherniack AD, Gupta M, Getz G, Gabriel SB, Meyerson M, Cibulskis C, Fei SS, Hinoue T, Shen H, Laird PW, Ling S, Lu Y, Mills GB, Akbani R, Loher P, Londin ER, Rigoutsos I, Telonis AG, Gibb EA, Goldenberg A, Mezlini AM, Hoadley KA, Collisson E, Lander E, Murray BA, Hess J, Rosenberg M, Bergelson L, Zhang H, Cho J, Tiao G, Kim J, Livitz D, Leshchiner I, Reardon B, Van Allen E, Kamburov A, Beroukhim R, Saksena G, Schumacher SE, Noble MS, Heiman DI, Gehlenborg N, Kim J, Lawrence MS, Adsay V, Petersen G, Klimstra D, Bardeesy N, Leiserson MDM, Bowlby R, Kasaian K, Birol I, Mungall KL, Sadeghi S, Weinstein JN, Spellman PT, Liu Y, Amundadottir LT, Tepper J, Singhi AD, Dhir R, Paul D, Smyrk T, Zhang L, Kim P, Bowen J, Frick J, Gastier-Foster JM, Gerken M, Lau K, Leraas KM, Lichtenberg TM, Ramirez NC, Renkel J, Sherman M, Wise L, Yena P, Zmuda E, Shih J, Ally A, Balasundaram M, Carlsen R, Chu A, Chuah E, Clarke A, Dhalla N, Holt RA, Jones SJM, Lee D, Ma Y, Marra MA, Mayo M, Moore RA, Mungall AJ, Schein JE, Sipahimalani P, Tam A, Thiessen N, Tse K, Wong T, Brooks D, Auman JT, Balu S, Bodenheimer T, Hayes DN, Hoyle AP, Jefferys SR, Jones CD, Meng S, Mieczkowski PA, Mose LE, Perou CM, Perou AH, Roach J, Shi Y, Simons JV, Skelly T, Soloway MG, Tan D, Veluvolu U, Parker JS, Wilkerson MD, Korkut A, Senbabaoglu Y, Burch P, McWilliams R, Chaffee K, Oberg A, Zhang W, Gingras M-C, Wheeler DA, Xi L, Albert M, Bartlett J, Sekhon H, Stephen Y, Howard Z, Judy M, Breggia A, Shroff RT, Chudamani S, Liu J, Lolla L, Naresh R, Pihl T, Sun Q, Wan Y, Wu Y, Jennifer S, Roggin K, Becker K-F, Behera M, Bennett J, Boice L, Burks E, Carlotti Junior CG, Chabot J, Prettida Cunha Tirapelli D, Sebastiãodos Santos J, Dubina M, Eschbacher J, Huang M, Huelsenbeck-Dill L, Jenkins R, Karpov A, Kemp R, Lyadov V, Maithel S, Manikhas G, Montgomery E, Noushmehr H, Osunkoya A, Owonikoko T, Paklina O, Potapova O, Ramalingam S, Rathmell WK, Rieger-Christ K, Saller C, Setdikova G, Shabunin A, Sica G, Su T, Sullivan T, Swanson P, Tarvin K, Tavobilov M, Thorne LB, Urbanski S, Voronina O, Wang T, Crain D , et al. 2017. Integrated genomic characterization of pancreatic ductal adenocarcinoma. *Cancer Cell* **32**:185–203 DOI 10.1016/j.ccell.2017.07.007.

Romero JM, Grünwald B, Jang G-H, Bavi PP, Jhaveri A, Masoomian M, Fischer SE, Zhang A, Denroche RE, Lungu IM, De Luca A, Bartlett JMS, Xu J, Li N, Dhaliwal S, Liang S-B, Chadwick D, Vyas F, Bronsert P, Khokha R, McGaha TL, Notta F, Ohashi PS, Done SJ, O'Kane GM, Wilson JM, Knox JJ, Connor A, Wang Y, Zogopoulos G, Gallinger S. 2020. A four-chemokine signature is associated with a t-cell–inflamed phenotype in primary and metastatic pancreatic cancer. *Clinical Cancer Research* **26**:1997–2010 DOI 10.1158/1078-0432.CCR-19-2803.

Ryan DP, Hong TS, Bardeesy N. 2014. Pancreatic adenocarcinoma. *New England Journal of Medicine* **371**:1039–1049 DOI 10.1056/NEJMra1404198.

Satija R, Farrell JA, Gennert D, Schier AF, Regev A. 2015. Spatial reconstruction of single-cell gene expression data. *Nature Biotechnology* **33**:495–502 DOI 10.1038/nbt.3192.

Sergeant G, Vankelecom H, Gremeaux L, Topal B. 2009. Role of cancer stem cells in pancreatic ductal adenocarcinoma. *Nature Reviews Clinical Oncology* **6**:580–586 DOI 10.1038/nrclinonc.2009.127.

Siegel RL, Miller KD, Fuchs HE, Jemal A. 2022. Cancer statistics, 2022. *CA: A Cancer Journal for Clinicians* **72**:7–33 DOI 10.3322/caac.21708.

Sohal DPS, Duong M, Ahmad SA, Gandhi NS, Beg MS, Wang-Gillam A, Wade JL, Chiorean EG, Guthrie KA, Lowy AM, Philip PA, Hochster HS. 2021. Efficacy of perioperative chemotherapy for resectable pancreatic adenocarcinoma: a phase 2 randomized clinical trial. *JAMA Oncology* **7(3)**:421–427 DOI 10.1001/jamaoncol.2020.7328.

Steele NG, Carpenter ES, Kemp SB, Sirihorachai VR, The S, Delrosario L, Lazarus J, Amir ED, Gunchick V, Espinoza C, Bell S, Harris L, Lima F, Irizarry-Negron V, Paglia D, Macchia J, Chu AKY, Schofield H, Wamsteker E-J, Kwon R, Schulman A, Prabhu A, Law R, Sondhi A, Yu J, Patel A, Donahue K, Nathan H, Cho C, Anderson MA, Sahai V, Lyssiotis CA, Zou W, Allen BL, Rao A, Crawford HC, Bednar F, Frankel TL, Pasca di Magliano M. 2020. Multimodal mapping of the tumor and peripheral blood immune landscape in human pancreatic cancer. *Nature Cancer* **1**:1097–1112 DOI 10.1038/s43018-020-00121-4.

Stein R, Mattes MJ, Cardillo TM, Hansen HJ, Chang C-H, Burton J, Govindan S, Goldenberg DM. 2007. CD74: a new candidate target for the immunotherapy of b-cell neoplasms. *Clinical Cancer Research* **13**:5556s–5563s DOI 10.1158/1078-0432.CCR-07-1167.

Suwa T, Kobayashi M, Shirai Y, Nam J-M, Tabuchi Y, Takeda N, Akamatsu S, Ogawa O, Mizowaki T, Hammond EM, Harada H. 2021. SPINK1 as a plasma marker for tumor hypoxia and a therapeutic target for radiosensitization. *JCI Insight* **6**:e148135 DOI 10.1172/jci.insight.148135.

Suzuki M, Shimizu T. 2019. Is SPINK1 gene mutation associated with development of pancreatic cancer? New insight from a large retrospective study. *EBioMedicine* **50**:5–6 DOI 10.1016/j.ebiom.2019.10.065.

Tanay A, Regev A. 2017. Scaling single-cell genomics from phenomenology to mechanism. *Nature* **541**:331–338 DOI 10.1038/nature21350.

Tang Z, Li C, Kang B, Gao G, Li C, Zhang Z. 2017. GEPIA: a web server for cancer and normal gene expression profiling and interactive analyses. *Nucleic Acids Research* **45**:W98–W102 DOI 10.1093/nar/gkx247.

Tempero MA, Malafa MP, Chiorean EG, Czito B, Scaife C, Narang AK, Fountzilas C, Wolpin BM, Al-Hawary M, Asbun H, Behrman SW, Benson AB, Binder E, Cardin DB, Cha C, Chung V, Dillhoff M, Dotan E, Ferrone CR, Fisher G, Hardacre J, Hawkins WG, Ko AH, LoConte N, Lowy AM, Moravek C, Nakakura EK, O'Reilly EM, Obando J, Reddy S, Thayer S, Wolff RA, Burns JL, Zuccarino-Catania G.

2019. Guidelines insights: pancreatic adenocarcinoma, version 1.2019. *Journal of the National Comprehensive Cancer Network* **17**:202–210 DOI 10.6004/jnccn.2019.0014.

Teng MWL, Ngiow SF, Ribas A, Smyth MJ. 2015. Classifying cancers based on t-cell infiltration and PD-L1. *Cancer Research* **75**:2139–2145 DOI 10.1158/0008-5472.CAN-15-0255.

Trapnell C, Cacchiarelli D, Grimsby J, Pokharel P, Li S, Morse M, Lennon NJ, Livak KJ, Mikkelsen TS, Rinn JL. 2014. The dynamics and regulators of cell fate decisions are revealed by pseudotemporal ordering of single cells. *Nature Biotechnology* **32**:381–386 DOI 10.1038/nbt.2859.

Uhlén M, Fagerberg L, Hallström BM, Lindskog C, Oksvold P, Mardinoglu A, Sivertsson Å, Kampf C, Sjöstedt E, Asplund A, Olsson I, Edlund K, Lundberg E, Navani S, Szigyarto CA-K, Odeberg J, Djureinovic D, Takanen JO, Hober S, Alm T, Edqvist P-H, Berling H, Tegel H, Mulder J, Rockberg J, Nilsson P, Schwenk JM, Hamsten M, von Feilitzen K, Forsberg M, Persson L, Johansson F, Zwahlen M, Heijne Gvon, Nielsen J, Pontén F. 2015. Tissue-based map of the human proteome. *Science* **347**:1260419 DOI 10.1126/science.1260419.

Vitale I, Manic G, Coussens LM, Kroemer G, Galluzzi L. 2019. Macrophages and metabolism in the tumor microenvironment. *Cell Metabolism* **30**:36–50 DOI 10.1016/j.cmet.2019.06.001.

Wang Z, Chen X, Liu N, Shi Y, Liu Y, Ouyang L, Tam S, Xiao D, Liu S, Wen F, Tao Y. 2021. A nuclear long non-coding RNA LINC00618 accelerates ferroptosis in a manner dependent upon apoptosis. *Molecular Therapy: The Journal of the American Society of Gene Therapy* **29**:263–274 DOI 10.1016/j.ymthe.2020.09.024.

Warburg O, Wind F, Negelein E. 1927. The metabolism of tumors in the body. *Journal of General Physiology* **8**:519–530 DOI 10.1085/jgp.8.6.519.

Winter JM, Brennan MF, Tang LH, D'Angelica MI, De Matteo RP, Fong Y, Klimstra DS, Jarnagin WR, Allen PJ. 2012. Survival after resection of pancreatic adenocarcinoma: results from a single institution over three decades. *Annals of Surgical Oncology* **19**:169–175 DOI 10.1245/s10434-011-1900-3.

Witkiewicz AK, McMillan EA, Balaji U, Baek G, Lin W-C, Mansour J, Mollaee M, Wagner K-U, Koduru P, Yopp A, Choti MA, Yeo CJ, McCue P, White MA, Knudsen ES. 2015. Whole-exome sequencing of pancreatic cancer defines genetic diversity and therapeutic targets. *Nature Communications* **6**:6744 DOI 10.1038/ncomms7744.

Xu Q, Chen S, Hu Y, Huang W. 2021a. Single-cell RNA transcriptome reveals the intra-tumoral heterogeneity and regulators underlying tumor progression in metastatic pancreatic ductal adenocarcinoma. *Cell Death Discovery* **7**:331 DOI 10.1038/s41420-021-00663-1.

Xu Q, Xu H, Deng R, Li N, Mu R, Qi Z, Shen Y, Wang Z, Wen J, Zhao J, Weng D, Huang W. 2021b. Immunological significance of prognostic alternative splicing signature in hepatocellular carcinoma. *Cancer Cell International* **21**:190 DOI 10.1186/s12935-021-01894-z.

Yao W, Maitra A, Ying H. 2020. Recent insights into the biology of pancreatic cancer. *EBioMedicine* **53**:102655 DOI 10.1016/j.ebiom.2020.102655.

Zhang AMY, Magrill J, de Winter TJJ, Hu X, Skovsø S, Schaeffer DF, Kopp JL, Johnson JD. 2019. Endogenous hyperinsulinemia contributes to pancreatic cancer development. *Cell Metabolism* **30**:403–404 DOI 10.1016/j.cmet.2019.07.003.